ACS NANO

www.acsnano.org

ARTICLE

Big Is Beautiful: Enhanced saRNA Delivery and Immunogenicity by a Higher Molecular Weight, Bioreducible, Cationic Polymer

Anna K. Blakney,[§] Yunqing Zhu,[§] Paul F. McKay, Clément R. Bouton, Jonathan Yeow, Jiaqing Tang, Kai Hu, Karnyart Samnuan, Christopher L. Grigsby, Robin J. Shattock,* and Molly M. Stevens*

Cite This: *ACS Nano* 2020, 14, 5711−5727

Read Online

ACCESS | Metrics & More | Article Recommendations | Supporting Information

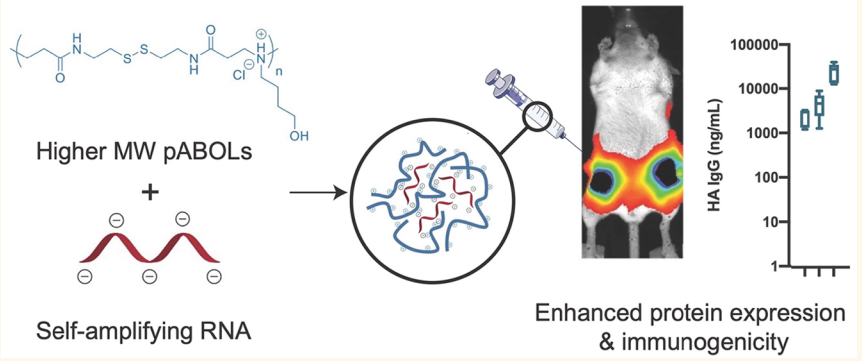

ABSTRACT: **Self-amplifying RNA (saRNA) vaccines are highly advantageous, as they result in enhanced protein expression compared to mRNA (mRNA), thus minimizing the required dose. However, previous delivery strategies were optimized for siRNA or mRNA and do not necessarily deliver saRNA efficiently due to structural differences of these RNAs, thus motivating the development of saRNA delivery platforms. Here, we engineer a bioreducible, linear, cationic polymer called "pABOL" for saRNA delivery and show that increasing its molecular weight enhances delivery both *in vitro* and *in vivo*. We demonstrate that pABOL enhances protein expression and cellular uptake *via* both intramuscular and intradermal injection compared to commercially available polymers *in vivo* and that intramuscular injection confers complete protection against influenza challenge. Due to the scalability of polymer synthesis and ease of formulation preparation, we anticipate that this polymer is highly clinically translatable as a delivery vehicle for saRNA for both vaccines and therapeutics.**

KEYWORDS: *RNA, replicon, polymer, vaccine, nucleic acid, influenza*

Due to progress in manufacturing and delivery, nucleic acids have emerged as an easily scalable and cost-effective vaccination strategy.[1,2] In addition to applications in protein replacement therapy, nucleic acids are a promising vaccine platform for both infectious diseases, such as HIV, influenza, and rabies, and cancer. Messenger RNA (mRNA) has several advantages as a nucleic acid platform compared to DNA; there is no risk of integration into the host genome, innate sensing can be modulated through base modifications and delivery vehicles, and it is the minimal genetic vector.[3−6] Furthermore, constructs targeting strain diversity or multiple infectious diseases can easily be combined.[7] Self-amplifying mRNA (saRNA), derived from the alphavirus genome,[8] is particularly advantageous as a vaccine platform, as it self-replicates upon delivery into the cytoplasm, which results in augmented protein expression and a minimum required dose of RNA.[9−11] However, because saRNA is a relatively large (~9500 nt), negatively charged molecule, it requires a delivery vehicle for efficient cellular uptake.

saRNA has previously been delivered using cationic emulsions,[12] lipid nanoparticles,[10] and polymers.[9,13] However,

Received: January 13, 2020
Accepted: April 8, 2020
Published: April 8, 2020

https://dx.doi.org/10.1021/acsnano.0c00326
ACS Nano 2020, 14, 5711−5727

Scheme 1. Schematic illustration of (a) improved aza-Michael addition to afford high molecular weight poly(amido amine)s, pABOLs (see Methods for details of 1 and 2) with molecular weights up to 167 kDa. (b) Complexation with self-amplifying RNA (saRNA) *via* a titration method and transfection efficacy of the pABOL-100 polyplexes, compared to jetPEI and PEI MAX.

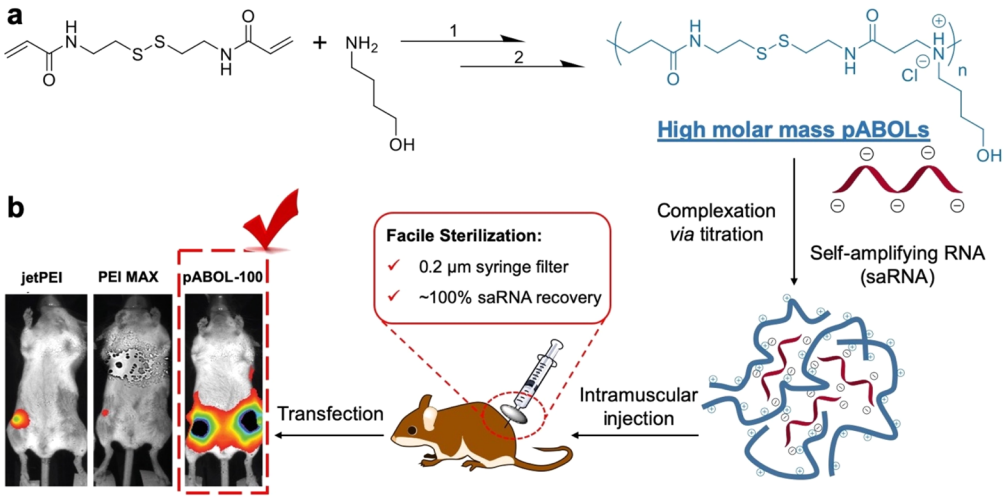

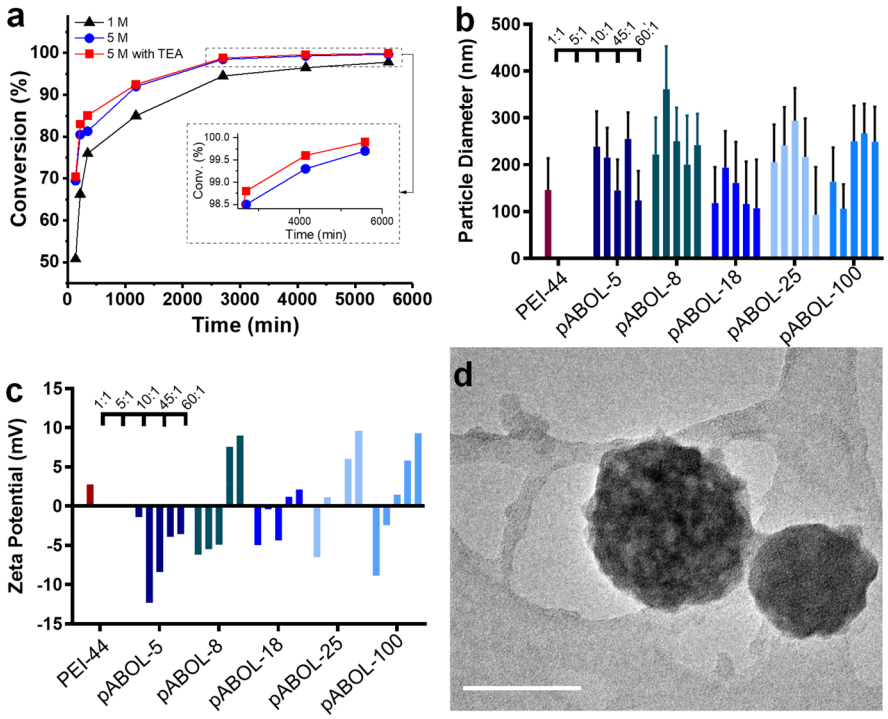

Figure 1. Synthesis of high MW pABOL and characterization of resulting saRNA polyplexes. (a) Polymerization kinetics of ABOL with CBA under different reaction conditions with varying monomer concentration, with and without triethylamine (TEA). The conversion values were calculated from the NMR integrals of double-bond signals at 5.60−6.23 ppm, using the methylene signals at 1.36−1.47 ppm as the internal reference. These methylene signals are assigned to g and h in Figure S2, which remain constant during the polyaddition (see Figure S4 for details). (b and c) Particle diameter and zeta potential of polyplexes formed *via* the direct mixing method between pABOLs and saRNA at polymer to saRNA weight ratios ranging from 1 to 45. PEI-44 [poly(ethylene imine), linear, 44 kDa] at a weight ratio of 5:1 was used as the reference. Bar represents mean ± SD for $n = 3$ with the weight ratio of polymer:saRNA indicated above the bars. (d) Typical TEM of polyplexes (pABOL-100/saRNA = 45:1, w/w) stained with 2 wt % uranyl acetate (scale bar: 100 nm; more images in Figure S6).

these delivery platforms were initially developed and optimized for shorter nucleic acids, such as siRNA (~20 nt) and mRNA (~2000−5000 nt), and we postulate that this may not be the optimal formulation for saRNA. We recently observed that the chain length and charge density of a commonly used cationic polymer, poly(ethylene imine) (PEI), strongly impacted *in vitro* transfection efficiency and that optimal polymers for mRNA and pDNA were not necessarily optimal for saRNA.[14] We hypothesized that this phenomenon would also be observed *in vivo*, however; increasing the molecular weight of PEI has previously been shown to have greater cytotoxicity.[15] We sought to use a cationic, linear

https://dx.doi.org/10.1021/acsnano.0c00326
ACS Nano 2020, 14, 5711−5727

polymer that is less cytotoxic at higher molecular weights to test whether increasing polymer molecular weight enhanced saRNA delivery *in vivo* without being confounded by cytotoxicity.

Poly(amido amine)s (pAMAMs) fit our polymeric criteria, and in addition, depending on the choice of monomer(s), linear pAMAMs generally have good water solubility, stability against hydrolysis, and tunable degradation.[16] The use of a disulfide monomer, *N,N′*-cystaminebis(acrylamide) (CBA), enables bioreduction *via* a disulfide backbone, which undergoes rapid cleavage intracellularly due to the presence of glutathione (GSH).[16] Furthermore, preparation of pAMAMs is simple; two monomers are mixed together and undergo aza-Michael polyaddition, which is a facile approach for scale-up and clinical translation. However, previous reports on pAMAMs have largely been limited to relatively low molecular weights of 5 to 20 kDa, which are oligomeric in nature.[16−22] Furthermore, systematic studies on the effect of molecular weight have been rare due to the difficulty in synthesizing high molecular weight pAMAMs.

Here, we prepared a library of poly(CBA-*co*-4-amino-1-butanol (ABOL)) (pABOL) polymers (Scheme 1) with varying molecular weights, ranging from 5 to 167 kDa, using an optimized aza-Michael polyaddition synthesis protocol. Using commercially available PEIs that have been used extensively *in vitro* and *in vivo* as a positive control,[23−27] we characterized the *in vitro* transfection efficiency and cytotoxicity. We then devised a method of polyplex preparation that enables the synthesis of monodisperse particles that are compatible with sterile filtration, which is imperative for clinical translation of this formulation. Furthermore, we quantified the relationship between pABOL molecular weight and protein expression *in vivo* using both intramuscular (IM) and intradermal (ID) injection. We then assessed whether protein expression was due to the quality or quantity of cellular expression *ex vivo* in human skin explants and *in vivo* in murine skin and muscle and observed the phenotype of cells in human skin that express pABOL/saRNA complexes. Finally, we use pABOL and hemagglutinin (HA)-encoding saRNA as a vaccine model and observe the immunogenicity and ability to protect against influenza challenge compared to PEI *in vivo*.

RESULTS AND DISCUSSION

Synthesis of pABOLs with High Molecular Weights. Bioreducible poly(amido amine)s, such as pABOL, have been used as polycations for the intracellular delivery of pDNA and mRNA[16] but previously have been synthesized up to a molecular weight of only ∼5−20 kDa. pABOLs are synthesized by aza-Michael polyaddition, which is a well-known method for making poly(amido amine)s. Here, we identify the required reaction conditions for preparation of higher molecular weight pABOLs. First, we increased the initial monomer concentration from 1.0 M to 5.0 M (defined as the CBA concentration), which led to a significant increase in reaction rate, reaching 98% of double-bond conversion after 2 days with a MW of 8.7 kDa (Figure S1a) in comparison with 4.9 kDa (conversion = 94%) observed at 1.0 M. However, due to the high viscosity, the reaction reached a kinetic barrier and higher molecular weights could not be achieved. To address this issue, triethylamine (TEA) was employed as a Lewis base catalyst to further increase the reaction rate. The addition of TEA increased the conversion by 0.2% in 4 days (Figure 1) and, importantly, resulted in a doubling of the molecular mass compared to the noncatalyzed reaction (Figure S1a). With the combination of higher monomer concentration and use of TEA as a catalyst, the targeted conversions (>99.5%) can be easily achieved within 3 days. The conversions were not monitored after 4 days, as the double-bond conversion exceeded 99.9% in the catalyzed reaction; thus, the residual signals were too weak to be detected *via* NMR spectroscopy. However, higher molecular weights are accessible by extending the reaction period from 5 to 14 days. pABOLs, with molecular weights ranging from 5 to 167 kDa (Table 1), were successfully prepared *via* the optimized aza-Michael polyaddition conditions (see Figures S2, S3, and S4 for NMR spectroscopy analyses with complete assignment of ^{1}H and ^{13}C NMR signals), which we refer to as pABOL-MW; for example, pABOL-8 has a MW of 8 kDa. Thus, though the *Đ* values were relatively high (Table 1) due to the fact that Michael addition polymerization is not a type of controlled polymerization, we were able to synthesize pABOLs with molecular weights of >30 kDa. Moreover, the method described here may be applicable for the synthesis of a broad range of high molecular weight pAMAMs given the widespread availability of commercial compounds capable of undergoing aza-Michael polyaddition.

Table 1. Characterization Data for pABOLs with Variable Molecular Weights

no.	polymers[a]	M_w(kDa)[b]	*Đ*[b]
1	pABOL-5[c]	5	1.7
2	pABOL-8	8	2.0
3	pABOL-18	18	2.5
4	pABOL-25	25	2.9
5	pABOL-33	33	4.6
6	pABOL-41	41	3.9
7	pABOL-72	72	5.9
8	pABOL-92	92	5.0
9	pABOL-100	105	6.4
10	pABOL-167	167	4.7

[a]Polymerization conditions: [CBA]/[ABOL]/[TEA] = 1.01/1/0.1, [CBA] = 5.0 M in MeOH/H_2O (4:1, v/v) at 45 °C, for 5 to 14 d under N_2 and in the dark (see SI for details). [b]Determined by size exclusion chromatography (SEC) in dimethylformamide (DMF) containing 0.075 wt % LiBr, at 40 °C, calibrated using monodisperse poly(methyl methacrylate) standards; [c]Polymerized without triethylamine (TEA) as the catalyst. See Figure S5 for SEC traces.

Increasing pABOL Molecular Weight Enhances Transfection Efficiency of Nucleic Acids *In Vitro*. In order to assess the effect of polymer molecular weight on complexation, the polyplexes were prepared *via* a direct mixing procedure. Given that the binding sites on both the saRNA and high molecular weight pABOLs might not be completely accessible, due to the higher-order structure and the sterically hindered tertiary amine groups, respectively, we have opted to use a range of polymer/RNA weight ratios (from 1:1 to 60:1) instead of the commonly used N/P values. It is noteworthy that theoretical average molecular weights per charge of pABOLs and saRNA are 349.5 and 339.5 g mol^{-1}, respectively, suggesting the weight ratios are close to N/P values (see Table S1 in the SI for the comparison between N/P values and weight ratios). When combined, pABOL and saRNA form nanoparticles with diameters ranging from 100 to

https://dx.doi.org/10.1021/acsnano.0c00326
ACS Nano 2020, 14, 5711−5727

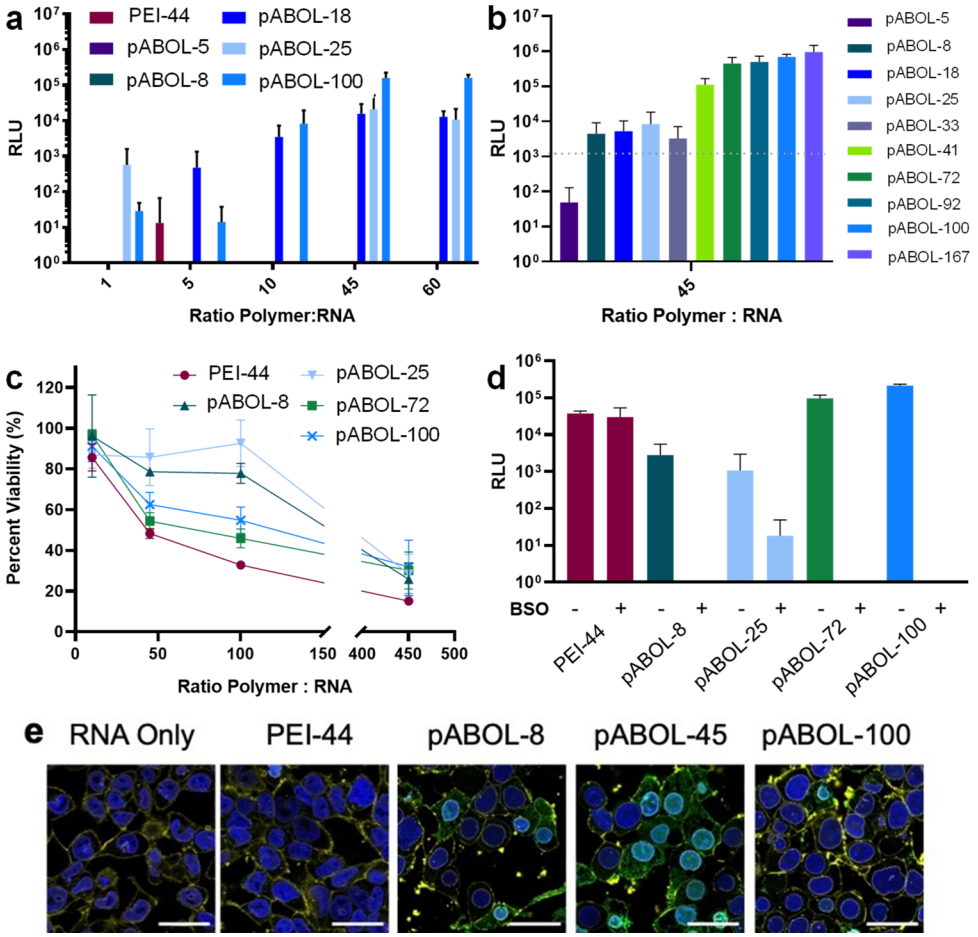

Figure 2. ***In vitro*** **transfection efficiency and cytotoxicity of pABOL polyplexes 24 h post-transfection. (a) Quantification of fLuc expression in relative light units (RLU) of polyplexes formed by PEI-44 and pABOLs with saRNA, 24 h after transfection at mass ratios of polymer:saRNA ranging from 1:1 to 45:1 (w/w) for** $n = 3$**. (b) Quantification of fLuc expression in RLU of polyplexes formed by all pABOLs in Table 1 at a mass ratio of 45:1 (see Figure S11 for other mass ratios) with** $n = 3$**. (c) Cytotoxicity studies of polyplexes formed at mass ratios ranging from 10:1 to 450:1 (saRNA loading = 100 ng), 24 h after initial transfection for** $n = 3$**. (d) Quantification of fLuc expression in RLU of polyplexes, using untreated cells (−) and cells (+) treated with glutathione (GSH) inhibitor, buthionine sulphoximine (BSO). Bar/dots represents mean ± SD,** $n = 3$**. (e) Confocal microscopy images of PEI and pABOL polyplexes after 1 h. Blue indicates nucleus (Hoescht), yellow indicates cell membrane (wheat germ agglutinin (WGA), Alexa Fluor 555 conjugate), and green indicates polymer (FITC). Scale bars = 20** μ**m.**

400 nm regardless of the weight ratios (Figure 1b). However, it is notable that only at weight ratios higher than 45:1 can nanoparticles formulated with pABOL above a molecular weight of 5 kDa exhibit sufficient positive surface charge to maintain adequate colloidal stability as well as good cell permeability (Figure 1c).[28] Furthermore, there is an apparent parabolic trend where molecular weights of 8, 25, and 100 kDa display a greater inflection in surface charge than 18 kDa pABOL. We observed that a polymer/RNA weight ratio of ≥10:1 (N/P = 8) was required to reach a neutral surface charge, which confirms our assumption that, due to the higher-order structure and steric hindrance, a certain number of binding sites between the amine groups on pABOL and the phosphate groups on the saRNA are left unbound during the polyplex formation. Furthermore, it takes less polymer loading to reach a positive surface charge for pABOLs with higher molecular weight. This is because polycations with higher molecular weight have more effective binding sites per chain, leading to the increase in binding constant between the polymer chains and saRNA[29] and consequently more polymer incorporated into nanoparticles and increased surface charge. These results indicate that higher molecular weight is favorable for reaching the desired surface charge with a lower polymer loading, which could also be beneficial for endosomal escape, as more tertiary amines per nanoparticle can serve as a proton sponge.[30] Transmission electron microscopy (TEM) was used to confirm the nanoparticle structure (Figures 1d, S6). The particle size (pABOL-100/saRNA = 45:1, w/w) shown in Figure 1d is smaller than the hydrodynamic diameter demonstrated in Figure 1b, which is commonly observed and attributed to skewing toward larger particle sizes when measured with dynamic light scattering (DLS) due to intensity-weighted values.

In order to evaluate the effect of pABOL molecular weight on the intracellular delivery of saRNA, we used saRNA encoding firefly luciferase (fLuc) as a reporter protein and indicator of transfection efficiency (Figure 2a). PEI is a polycation that is widely used for nucleic acid transfection and thus serves as a positive control.[31] At weight ratios below 10:1, there was no effect of increasing the molecular weight, likely because of the surface charge being negative or neutral, as shown in Figure 1c, which is unfavorable for cell uptake or

https://dx.doi.org/10.1021/acsnano.0c00326
ACS Nano 2020, 14, 5711−5727

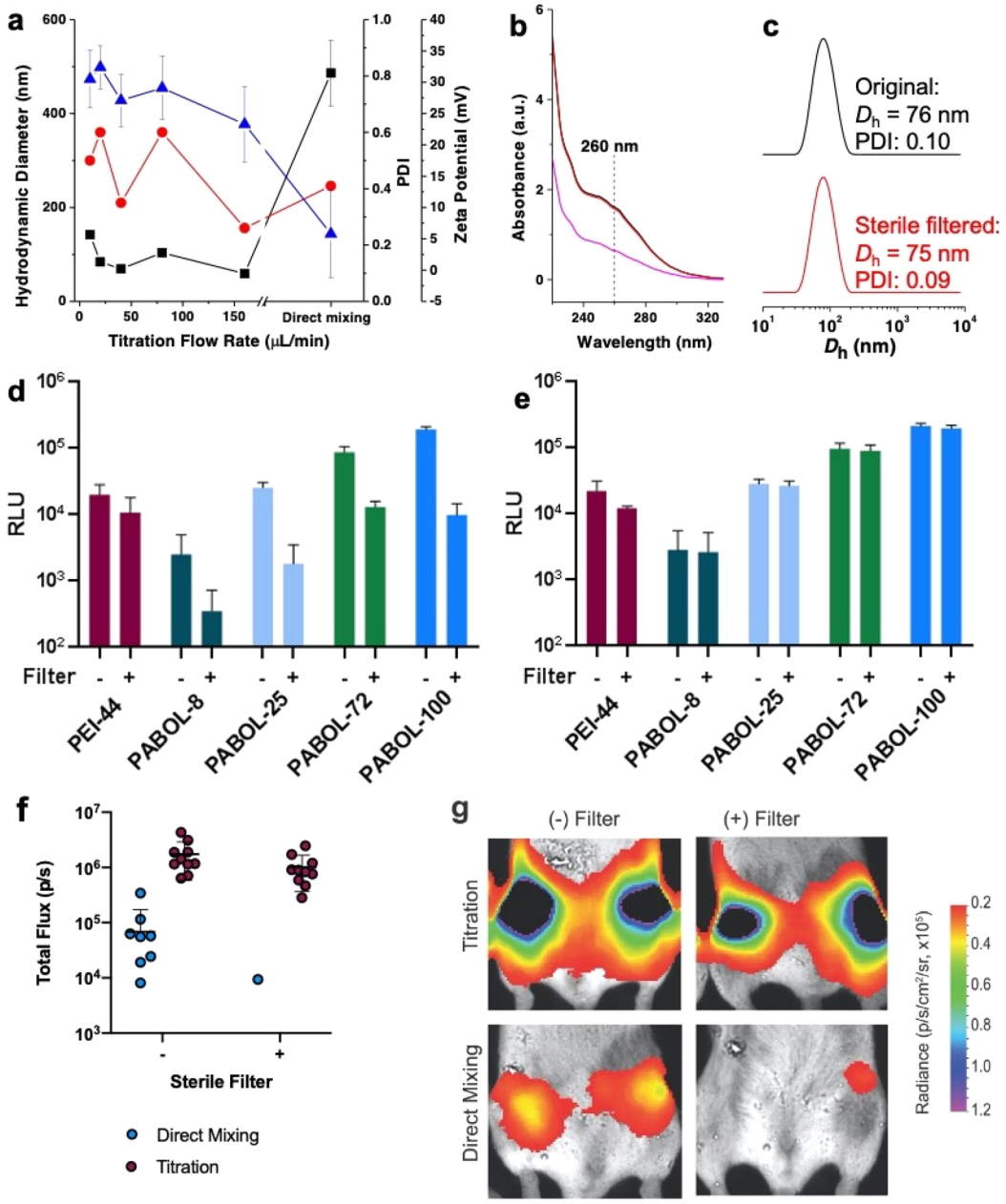

Figure 3. Functional characterization of polyplexes prepared using either the direct addition or titration methods *in vitro* and *in vivo*. (a) Hydrodynamic diameter (black squares), polydispersity (red circles), and zeta potential (blue triangles) of polyplexes formed *via* the titration method (adding saRNA to polymer) at various titration flow rates (from 10 to 160 μL min^{-1}), using pABOL-100 (polymer/RNA = 45:1, w/w). Data from the direct mixing method is included for reference. (b) Absorbance curves of polyplexes measured by Nanodrop before (black) and after (red) passing through a 0.2 μm syringe filter (pink curve: absorbance of pABOL-100 in buffer with the same concentration as in the obtained polyplex solution). (c) Hydrodynamic diameter of polyplexes measured by DLS before (black) and after (red) passing through a 0.2 μm syringe filter. (d and e) Quantification of fLuc expression in RLU, using filtered (+) and nonfiltered (−) polyplexes formed *via* the direct mixing and titration method, respectively. Bar represents mean ± SD, n = 3. (f) Quantification of fLuc expression of filtered or nonfiltered pABOL polyplexes formed by direct addition and titration methods, 7 d after injection. Mice were injected with 5 μg of saRNA in each leg and a ratio of polymer to RNA of 45:1 (w/w) for pABOL. Each circle represents one leg of one animal, and bar represents mean ± SEM, n = 10. (g) Representative images of each group, corresponding to (f).

colloidal stability. However, at weight ratios ≥ 45:1, the transfection efficiency shows a molecular weight dependence: higher molecular weights promote higher transfection efficacy. To investigate further, additional *in vitro* tests were conducted using pABOLs with a wider range of molecular weights at a weight ratio of 45:1 (Figure 2b). The results confirm the molecular weight dependence, but also suggest nonmonotonic behavior. At molecular weights below 72 kDa, higher molecular weight is indeed preferable. However, the transfection efficiency reaches a plateau for pABOLs with molecular weight between 72 and 167 kDa. Considering the added time it takes to increase the molecular weight from 100 to 167 kDa during polymerization and negligible impact on transfection efficacy, there is no advantage in increasing the molecular weight beyond 100 kDa.

https://dx.doi.org/10.1021/acsnano.0c00326
ACS Nano 2020, 14, 5711−5727

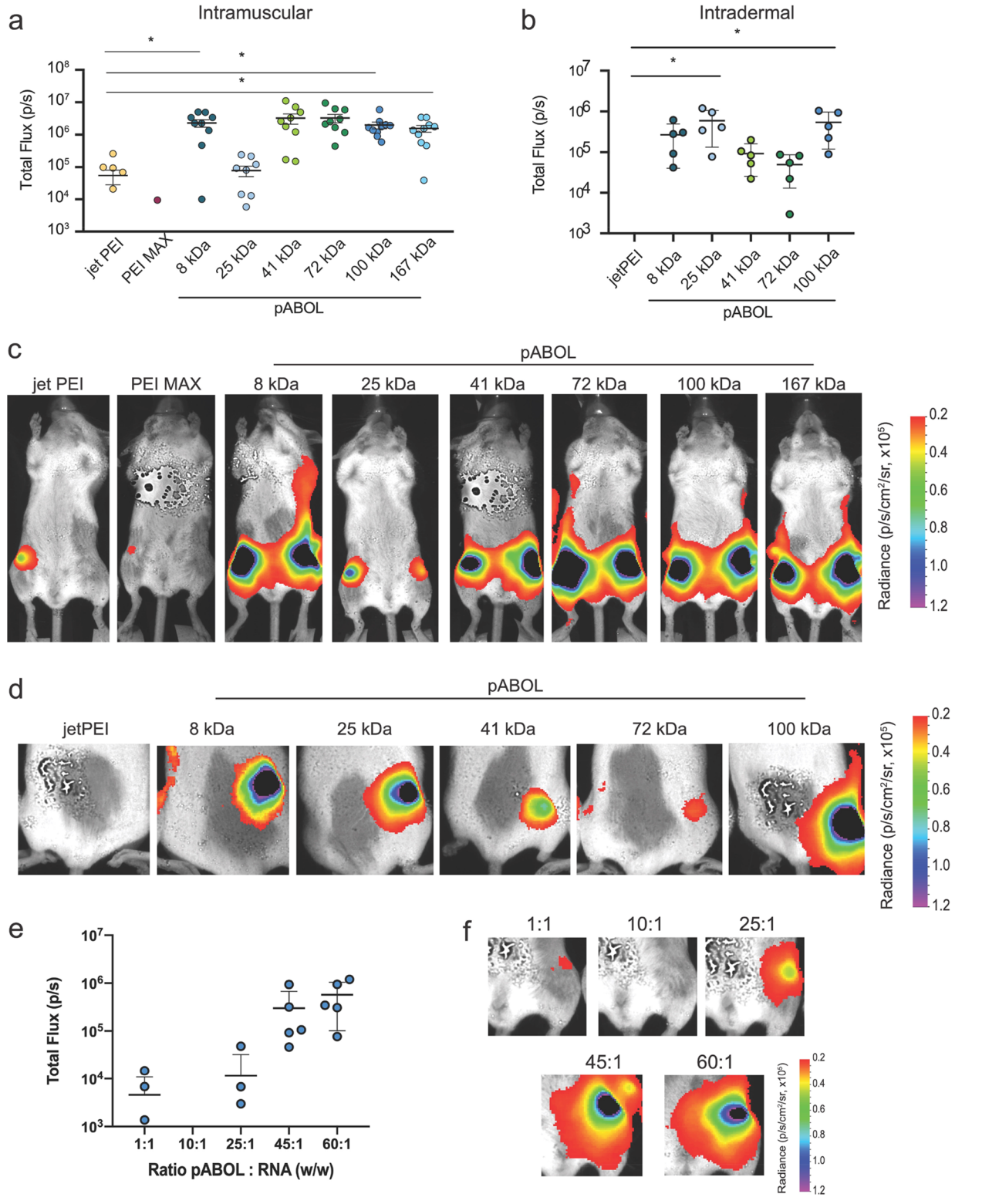

Figure 4. Effect of molecular weight, route of administration, and ratio of pABOL to RNA on *in vivo* expression of fLuciferase-encoding saRNA polyplexes. (a, b) Quantification of fLuc expression of PEI (jetPEI and PEI MAX) and pABOL polyplexes in total flux (p/s), 7 d after injection. Mice were injected with 5 μg of saRNA either intramuscularly (a) or intradermally (b), and a polymer to RNA ratio of 45:1 (w/w) for pABOL, 1:1 for PEI MAX, and an N:P of 8 for jetPEI. Each circle represents one leg of one animal, and bar represents mean ± SD, n = 5. (c, d) Representative images of each group after IM (c) and ID (d) injection. (e) Quantification of fLuc expression *in vivo* 7 d after IM injection of 5 μg of saRNA with varying ratios of pABOL to RNA. Each circle represents one leg of one animal, and bar represents mean ± SD, n = 5. (f) Representative images of each group, corresponding to (e). *Indicates significance based on a one-way ANOVA with $p < 0.05$.

https://dx.doi.org/10.1021/acsnano.0c00326
ACS Nano 2020, 14, 5711−5727

We also tested whether increasing the molecular weight of pABOL or the formulation buffer similarly enhanced the transfection efficiency of mRNA and plasmid DNA (pDNA) (Figures S7, S8, and S9). Although the enhancement in mRNA and pDNA transfection was not as significant as for saRNA, it implies the molecular weight effect is specifically applied not only to long-chain nucleic acids, like saRNA, but to other nucleic acid species as well. This knowledge is useful for the future design of polymer-based delivery systems for nucleic acids.

In addition to transfection efficiency, we also evaluated the *in vitro* cytotoxicity of saRNA/pABOL formulations (Figure 2c). Compared to PEI, pABOLs display less cytotoxicity. Furthermore, a molecular weight dependence was observed for pABOLs. pABOLs with low/moderate molecular weights (8 and 25 kDa) demonstrate much less cytotoxicity, compared to their high molecular weight analogues (72 and 100 kDa), which could be due to surface charge and/or the concentration of free polycations. Further characterization of the pABOL/saRNA polyplexes was carried out using Limulus Amebocyte Lysate (LAL) testing; all polyplex formulations were found to have endotoxin levels of $<0.25 \pm 0.005$ EU/mL.

We then sought to determine the role of bioreduction of pABOLs on *in vitro* transfection efficiency. As a bioreducible polycation, it is hypothesized that pABOL releases saRNA *via* the intracellular GSH reduction of the disulfide bonds on its backbone.[16] To confirm that pABOL is capable of being reduced by GSH, the bioreduction of pABOLs was monitored using GSH, and the reduced product was identified to be a dithiol compound (see Figure S10a for its chemical structure). We then used a known GSH inhibitor, buthionine sulphoximine (BSO),[32] to pretreat cells and evaluate whether pABOLs had the same transfection with normal or reduced intracellular levels of GSH. All pABOL polyplexes showed a significant decrease in transfection efficiency following BSO pretreatment (Figure 2d). PEI, which is not bioreducible, showed no decrease in transfection efficiency, indicating that BSO pretreatment did not impact the ability of the cells to express luciferase and that GSH is integral in decomplexation of pABOL. This agrees with previous reports that the bioreducibility of pABOL accelerates the decomplexation with other nucleic acids.[18,33] This may be particularly relevant for self-amplifying RNAs, where the fast release mechanism delivered by pABOLs may facilitate rapid transgene expression.

Finally, we utilized FITC-labeled PEI and pABOL to visualize the uptake of saRNA polyplexes in HEK cells *in vitro* (Figure 2e). Both PEI and pABOL polyplexes were observed to be internalized by 1 h post-transfection, in agreement with the protein expression observed in Figure 2a,b. Overall, we observed that increasing the molecular weight of pABOL from 5 kDa to 100 kDa enhances saRNA transfection efficiency *in vitro* in a bioreduction-dependent manner and that pABOL enables higher transfection efficiency and lower cytotoxicity compared to commercially available PEI.

Optimization of pABOL/saRNA Complexation Procedure for Sterile Filtration. In order to facilitate downstream product sterilization, it is imperative to develop saRNA-polyplexes that can undergo filter sterilization (0.2 μm) without loss of activity. To address this issue, we optimized a titration method to prepare polyplexes with a size of <100 nm. Titrating saRNA solutions (800 μL, 1.00×10^{-3} mg mL^{-1}) into polymer solutions (200 μL, 0.18 mg mL^{-1}) at a flow rate of 160 μL min^{-1} yields smaller nanoparticles with a hydrodynamic diameter of ~70 nm, narrow dispersity (0.2), and high surface charge (+ 23 mV) (Figures 3a, S12). Increasing the weight ratio from 45:1 to 60:1 did not influence particle sizes (Figure S13). We found that a hydrodynamic diameter of ~70 nm is sufficiently small enough for sterile filtration without losing any nanoparticles (Figure S14). The titration method was found to form consistent particles despite the molecular weight of pABOL or the ratio of pABOL to saRNA, which is likely due to the controlled addition of RNA to the polymer, allowing for more even interaction between the polymer and RNA compared to the direct mixing method (Figure S15). The saRNA recovery after sterile filtration was monitored using the UV absorbance of the RNA at 260 nm (Figure 3b). RNA concentrations before (black) and after (red) filtration were identical, as was the hydrodynamic diameter (Figure 3c), suggesting no saRNA loss during sterile filtration.

In order to demonstrate that polyplexes formed by the titration method enable high transfection efficiency even after sterile filtration, we evaluated sterile filtered particles *in vitro* and *in vivo*. Polyplexes prepared using direct mixing were used as the control. While the transfection efficiency of polyplexes formed by direct mixing decreased by at least 1 order of magnitude (Figure 3d) after sterile filtration, the titrated polyplexes were not affected at all (Figure 3e), suggesting that nanoparticles of ~70 nm and narrow dispersity are favorable for sterile filtration. A similar phenomenon was also observed *in vivo*; polyplexes formed *via* titration had high luciferase expression (~10^6 p/s) both before and after sterile filtration, while the ones generated by direct mixing had slightly lower luciferase expression (~10^5 p/s) and were no longer effective after sterile filtration (Figure 3f and g). Thus, we conclude that the titration method could facilitate scalable production of pABOL/saRNA polyplexes that facilitate protein expression both *in vitro* and *in vivo*. This approach would be highly amenable to the use of scale up processes such as automated microfluidics for in-line mixing and downstream tangential flow filtration to provide greater particle homogeneity prior to sterile filtration.

Increasing pABOL Molecular Weight Enhances Luciferase Expression *In Vivo*. We further investigated whether increasing the molecular weight of pABOLs enhanced the delivery and expression of saRNA *in vivo*, using fLuc as a reporter protein (Figure 4). We tested a range of pABOL molecular weights, from 8 to 167 kDa, as these were the polymers that we found to effectively complex and condense saRNA (Figure 1b and c). Mice were injected with 5 μg of fLuc saRNA prepared at a polymer:saRNA ratio of 45:1 (w/w) either IM or ID and imaged after 7 d, which has been previously shown to be peak protein expression for Venezuelan equine encephalitis virus (VEEV).[13] We used two commercially available linear PEIs as positive controls: PEI MAX, which was used in all of our transfection experiments, and *in vivo* jetPEI, which has previously been shown to more effectively deliver RNA *in vivo*.[34] We observed signal from only one leg of one mouse in the PEI MAX IM group, whereas the average of the jetPEI group was 8×10^4 p/s (Figure 4a), confirming that jetPEI is a more effective *in vivo* delivery agent for RNA. We observed similar superiority of pABOL polyplexes *in vivo* to those for the *in vitro* experiments: the 8, 41, 72, 100, and 167 kDa pABOLs had an

https://dx.doi.org/10.1021/acsnano.0c00326
ACS Nano 2020, 14, 5711−5727

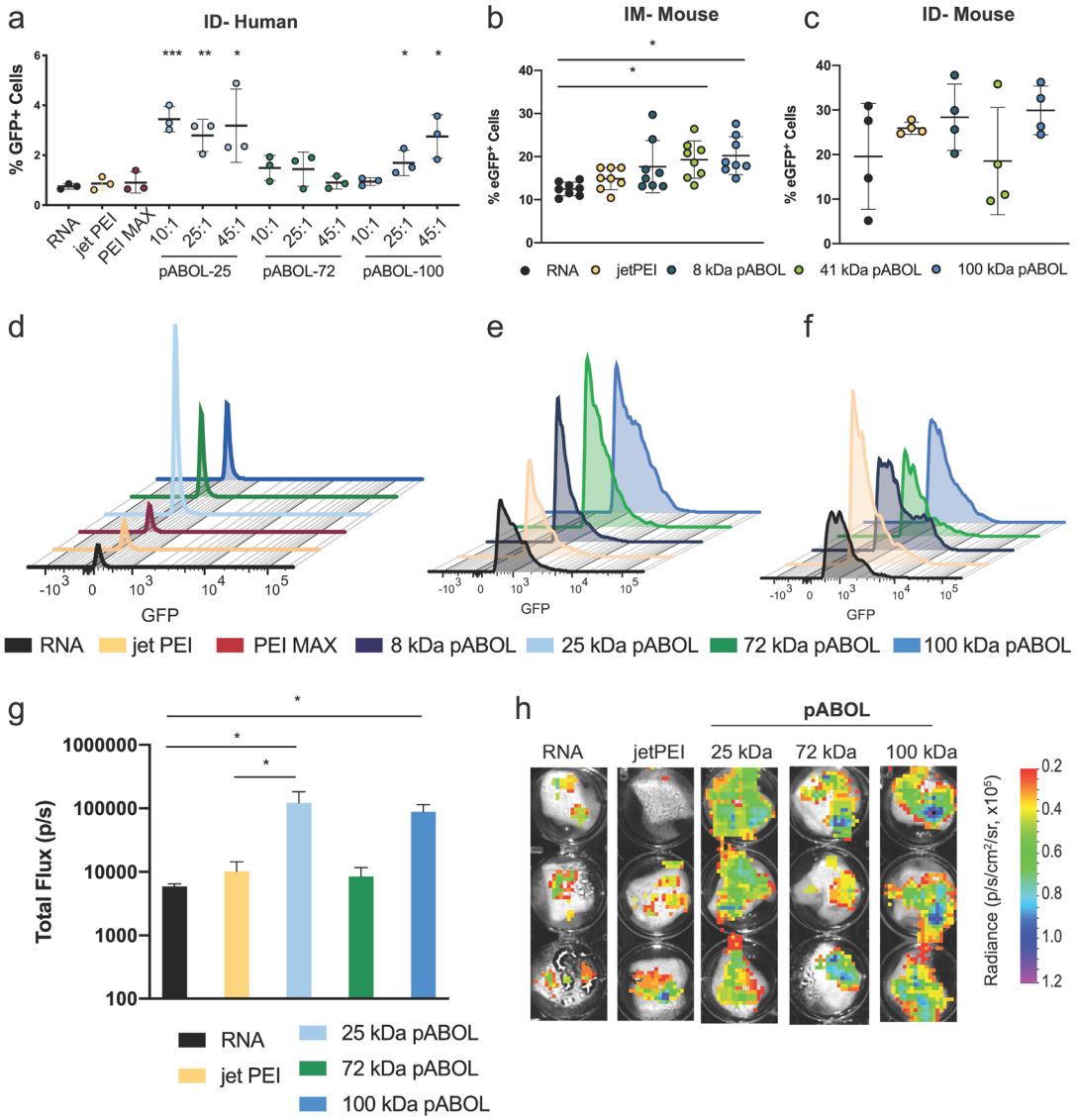

Figure 5. Cellular expression of saRNA after IM (mouse) or ID (human, mouse) injection with polyplex formulations. (a) Percentage of eGFP+ cells out of total live cells for each formulation after an intradermal injection of 2 μg of saRNA in human skin explants. Explants were analyzed 72 h after initial injection. jetPEI and PEI MAX were formulated at ratios of N/P = 8 and 1, respectively. pABOL formulations were prepared at ratios of 10:1, 25:1, and 45:1. Bars represent mean ± SD for n = 3, with *, **, and * indicating significance of $p < 0.05$, 0.01, and 0.001 using an unpaired, two-tailed t test, respectively. (b, c) Percentage of eGFP+ cells out of total live cells for each formulation after either IM (b) or ID (c) injection of 5 μg of saRNA in mice. Tissue was excised 7 d after initial injection. jetPEI was formulated at a ratio of N/P = 8, and pABOL formulations were prepared at a ratio of 45:1. Bars are mean ± SD for n = 8 (IM) and 4 (ID), with * indicating significance of $p < 0.05$ using an unpaired, two-tailed t test. (d–f) Histograms of mean eGFP fluorescence intensity (MFI) for each formulation in human skin explants (d), IM injection in mice (e), and ID injection in mice (f). (g) fLuc expression of human skin explants after ID injection with 2 μg of saRNA. Explants were analyzed 72 h after initial injection. Bars represent mean ± SD for n = 3, with * indicating significance of $p < 0.05$ using an unpaired, two-tailed t test. (h) Representative images corresponding to (g).**

average luciferase expression of 5×10^6 p/s when injected IM, ~62-fold higher than the jetPEI group. Interestingly, the 25 kDa pABOL had equivalent luciferase expression (~10^5 p/s) to jetPEI when injected IM, resulting in a parabolic relationship between pABOL molecular weight and luciferase expression *in vivo*. The 8, 100, and 167 kDa groups had statistically significantly higher luciferase expression than the jetPEI when injected IM, with $p = 0.0446$, 0.0332, and 0.0354, respectively. There was no signal from the ID jetPEI group (Figure 4b), however; the pABOL ID mice had similarly high luciferase expression to the IM groups, and we again observed a parabolic relationship between expression and molecular weight. The 8, 25, and 100 kDa groups had a luciferase expression of ~10^6 p/s, while the 41 and 72 kDa groups had a luciferase expression of ~10^5 p/s. However, only the 25 and 100 kDa groups were statistically significantly higher, with $p = 0.0093$ and 0.0186, respectively. We postulate that this parabolic relationship is governed by a mechanism wherein high luciferase expression from the 8 kDa pABOL polyplexes results from more rapid reduction and thus rapid uptake of RNA *in vivo*, whereas the higher molecular weight polymers are reduced less quickly but provide more adequate protection for the RNA, potentially resulting in high intracellular RNA delivery. Thus, the pABOLs with moderate molecular weight

https://dx.doi.org/10.1021/acsnano.0c00326
ACS Nano 2020, 14, 5711–5727

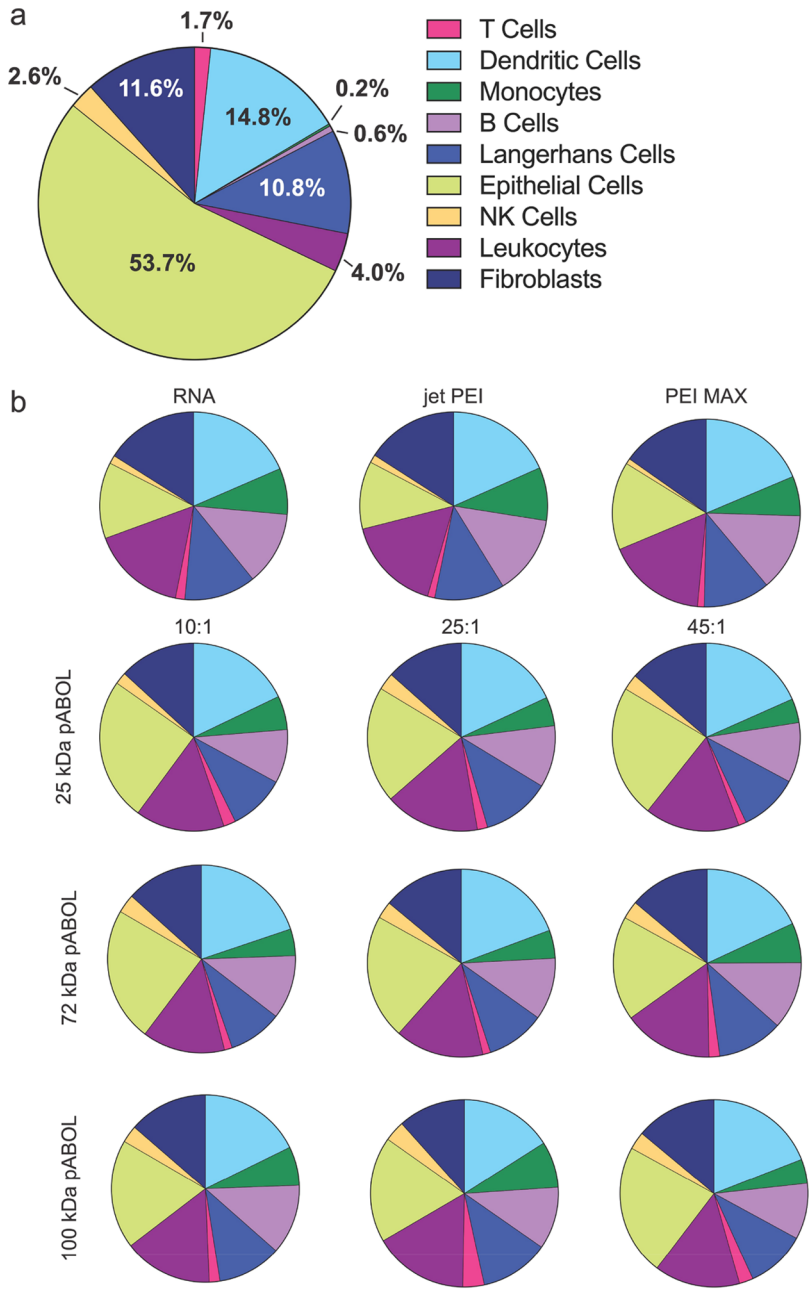

Figure 6. Phenotypic identity of cells present in human skin explants and GFP+ cells after intradermal (ID) injection of polyplex formulations as determined by flow cytometry. (a) Identity of cells in the population of total cells extracted from human skin explants. (b) Identity of GFP-expressing skin cells from explants treated with polyplex-formulated eGFP-encoding saRNA. Cells identified using the following antibodies: epithelial cells (CD45−), fibroblasts (CD90+), NK cells (CD56+), leukocytes (CD45+), Langerhans cells (CD1a+), monocytes (CD14+), dendritic cells (CD11c+), T cells (CD3+), and B cells (CD19+).

(25 and 41 kDa), which theoretically are reduced less quickly, may provide less adequate RNA protection, resulting in lower signal and more variability of protein expression *in vivo*.

Finally, we sought to determine the optimal ratio of pABOL to saRNA *in vivo* (Figure 4e,f). We used ratios of 1:1 to 60:1 with pABOL-100 and observed that ratios of ≤25:1 yielded luciferase expression of 10^4 p/s or less. However, with a ratio of 45:1 the luciferase expression increased to ∼10^6 p/s and there was no added benefit of increasing the ratio to 60:1. We observed that increasing the molecular weight of a cationic, bioreducible polymer enhances protein expression from saRNA *in vivo*. Our results are similar to trends previously observed for saRNA *in vitro*.[14] The increased level of expression mediated by pABOL relative to PEI suggested a potential advantage for the delivery of saRNA biotherapeutics.

pABOL Enhances the Quantity of Cells Expressing saRNA Both *In Vivo* and *Ex Vivo* in Human Skin Explants. After observing efficient saRNA delivery *in vivo*, we then sought to investigate whether pABOLs enhance the quality or quantity of cells expressing saRNA both *ex vivo* in a clinically relevant human skin explant model and *in vivo* in mouse muscle and skin. For the skin explants, we compared saRNA alone, the commercially available PEIs (PEI MAX and jetPEI), and 25, 72, and 100 kDa pABOL complexed with 2 μg of enhanced green fluorescent protein (eGFP) saRNA (Figure 5a,d). RNA alone resulted in eGFP expression in ∼1%

https://dx.doi.org/10.1021/acsnano.0c00326
ACS Nano 2020, 14, 5711−5727

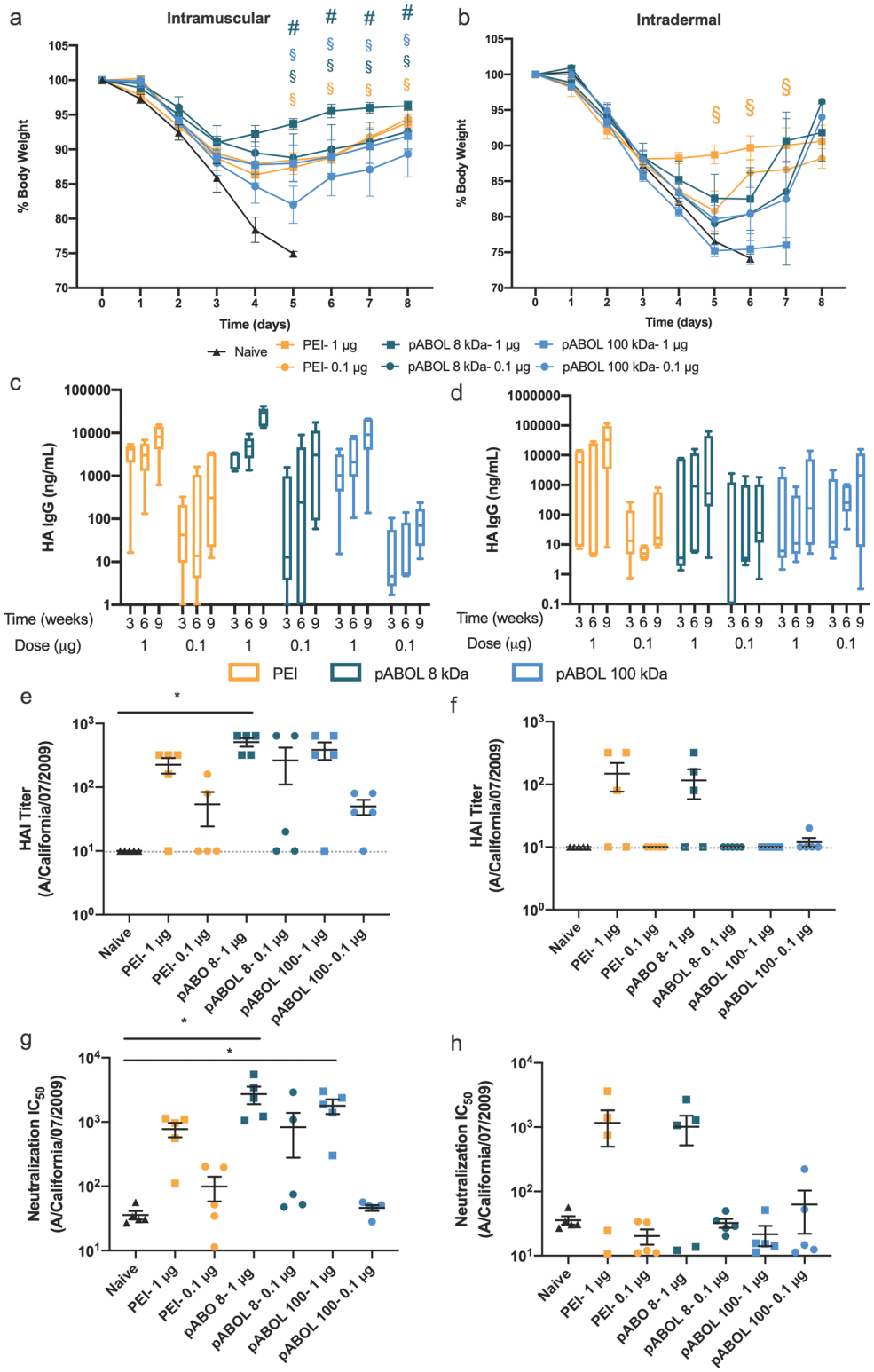

Figure 7. Immunogenicity of HA-encoding saRNA polyplexes. (a, b) Change in body weight after IN challenge with Cal/09 flu virus for mice injected either IM (a) or ID (b). Dots represent mean percentage, normalized to day 0 for each mouse, ±SEM for $n = 5$. § indicates significance of $p < 0.05$ for 1 μg dose *vs* naïve, while # indicates significance of $p < 0.05$ for 1 μg dose PEI group *vs* 1 μg dose pABOL group as evaluated using multiple *t* tests adjusted for multiple comparisons. (c, d) HA antigen-specific IgG antibody titers following immunization with prime and boost of saRNA complexed with jetPEI, 8 kDa pABOL, or 100 kDa pABOL for mice injected either IM (c) or ID (d). Data are presented as box and whiskers with outer limits of the minimum and maximum, and a line as the mean for $n = 5$. (e, f) HAI titer of Cal/09 flu virus for mice injected either IM (e) or ID (f). Gray dotted line represents the limit of detection. (g, h) Neutralization IC_{50} against Cal/09 flu virus for mice injected either IM (g) or ID (h). * indicates significance of $p < 0.05$ as evaluated using a Kruskal–Wallis test with multiple comparisons. Each bar represents mean ± SEM for $n = 5$ at each time point.

https://dx.doi.org/10.1021/acsnano.0c00326
ACS Nano 2020, 14, 5711−5727

of human skin cells (Figure 5a), and complexation with PEI MAX and jetPEI did not increase the number of eGFP-positive cells. However, the 25 kDa pABOL complexed with saRNA at a ratio of 10:1, 25:1, and 45:1 (w/w) increased the number of eGFP-positive cells to 3%, significantly higher than the RNA alone (p = 0.0080, 0.0056, and 0.0457, respectively). Interestingly, the 72 kDa pABOL did not increase the number of eGFP-positive cells at any of the ratios tested, but the 100 kDa pABOL resulted in 1.5% and 2.5% eGFP-positive cells at ratios of 25:1 and 45:1 (p = 0.0346 and 0.0170, respectively). We then sought to characterize whether the formulations were enhancing the amount of protein expression per cell (quality of expression), as evidenced by quantifying the median fluorescence intensity (MFI) (Figure 5d). RNA alone had an eGFP MFI of $\sim 10^2$, and none of the formulations enhanced the protein expression per cell, which would manifest as a shift to the right on the x-axis of the histogram plot in Figure 5d. It is hypothesized that this is due to the self-replicating nature of the VEEV vector, reaching a maximal level of GFP expression and thus MFI per cell.

We then tested whether increasing the molecular weight of pABOL enhanced the number of cells expressing eGFP after IM and ID injection in mice (Figure 5b,c). We observed that RNA alone yielded expression in ∼10% of cells when injected IM, which was only enhanced to ∼20% of cells by 41 and 100 kDa pABOL (p = 0.0074 and 0.0022, respectively). pABOL of 8 kDa enhanced the eGFP+ cells to 16%, but this was not statistically significant. Similarly, we observed that RNA alone yielded eGFP expression in 20% of cells after ID injection, which was increased to ∼30% of cells with 8 and 100 kDa pABOL, although the differences were not statistically significant. jetPEI and 41 kDa pABOL did not enhance the number of eGFP+ cells when injected ID. We postulate that this is due to differential cell types between the muscle and the skin, which may have different kinetics of pABOL reduction and saRNA expression. Similar to the human skin explants, there was no significant shift in GFP MFI (Figure 5e,f), further indicating that the total protein expression relies on the number of cells and not the amount of protein being expressed by each cell. These results directly reflect the relationship between pABOL molecular weight and luciferase expression *in vivo*, demonstrated in Figure 4.

While the 25 kDa pABOL resulted in ∼4% of eGFP-positive cells in human skin explants, this is a relatively low transfection efficiency. Although this strongly agrees with the *in vivo* RNA expression levels that Liang *et al.* observed after intramuscular and intradermal mRNA injection in rhesus macaques,[35] we sought to determine whether this correlated with luciferase expression in human skin explants. We injected human skin explants with 2 μg of fLuc saRNA complexed with jetPEI and 25, 72, or 100 kDa pABOL at a mass ratio of 45:1 (w/w). Indeed, the 25 and 100 kDa pABOL polyplexes had the highest luciferase expression (100 000 p/s), which directly reflects the percentage of eGFP+ cells in Figure 5a. Overall, we found that pABOL enhances the percentage of cells expressing saRNA compared to RNA alone or commercially available PEIs when injected IM or ID *in vivo* in mice or ID *ex vivo* in human skin explants.

pABOL-Delivered saRNA Is Preferentially Expressed by Epithelial Cells in Human Skin Explants. We then further investigated which cells in human skin explants were expressing eGFP saRNA after intradermal injection (Figure 6). We observed that human skin explants are composed primarily of epithelial cells (53.7%), dendritic cells (14.8%), fibroblasts (11.6%), and Langerhans cells (10.8%) (Figure 6a). The remaining 9% is composed of more rare immune cells, including leukocytes (4.0%), natural killer (NK) cells (2.6%), T cells (1.7%), B cells (0.6%), and monocytes (0.2%). Despite the predominance of epithelial cells in the skin when injected alone, saRNA was expressed in dendritic cells (DCs) (18.5%), leukocytes (16.3%), fibroblasts (16.0%), epithelial cells (13.1%), B cells (12.7%), Langerhans cells (12.3%), monocytes (8.0%), T cells (1.6%), and NK cells (1.4%) (Figure 6b). There was a similar trend in cell types for both PEI MAX and jetPEI formulations. However, for all of the pABOL polyplexes, epithelial cells were the dominant cell type expressing the saRNA (18−24%), followed by DCs, leukocytes, Langerhans cells, B cells, fibroblasts, monocytes, NK cells, and T cells. We hypothesize that the predominant uptake of RNA alone and PEI-complexed RNA by mostly immune cells indicates that these formulations are scavenged by professional immune cells, whereas the pABOL formulations may actively affect cellular uptake into epithelial cells. These findings are similar to characterization by Liang *et al.*, where cells express the mRNA encapsulated in lipid nanoparticle formulations when injected intradermally in rhesus macaques.[35] In that study they did not characterize the same cell types but found that the formulations were mostly taken up by and expressed in monocytes and DCs. It is unknown whether the total number or the phenotype of cells that express saRNA affects the immunogenicity of a vaccine. However, here we show that formulating saRNA with pABOL results in uptake by a more diverse array of human skin cells compared to RNA alone or commercially available PEIs.

Hemagluttinin saRNA/pABOL Polyplexes Induce High HA Antibody and Neutralization Titers and Confer Complete Protection against Influenza Virus Challenge *In Vivo*. We then sought to assess the immunogenicity and protective capacity of HA-encoding saRNA delivered by pABOL, when injected either IM or ID (Figure 7). Mice received a prime and boost of either 1 or 0.1 μg of saRNA complexed with either jetPEI, 8 kDa pABOL, or 100 kDa pABOL at a polymer to saRNA ratio of 45:1 (w/w). The boost was administered 6 weeks after the initial prime. The mice were challenged intranasally (IN) with a Cal/09 influenza virus 3 weeks after the boost and weighed daily to monitor disease pathology. A relatively high dose of 4.2×10^5 pfu was used in order to discriminate weight loss between groups. The naïve mice in both the IM and ID groups all lost >25% of their body weight between days 4−6 and had to be euthanized according to the challenge protocol humane endpoints (Figure 7a,b). In the IM injection groups, all mice in the PEI and 8 kDa pABOL groups were completely protected, even in the 0.1 μg groups, with the 1 μg 8 kDa pABOL group showing the least amount of weight loss at peak viremia (∼8%). All the mice in the 1 μg 100 kDa pABOL group were completely protected, but two mice in the 0.1 μg 100 kDa pABOL group reached 25% weight loss on day 5 and had to be euthanized, thus resulting in 60% survival in this group (Figure S16a). The HA IgG antibody titers (Figure 7c,d) directly reflect the challenge results; all groups show increasing antibody titers between 3 and 6 weeks and then after the boost. The 1 μg 8 kDa pABOL group had the highest antibody titers (∼40 000 ng/mL) after 9 weeks, whereas the PEI and 100 kDa pABOL groups that received 1 μg were equivalent (∼10 000 ng/mL). Even after 9 weeks, the 0.1 μg

https://dx.doi.org/10.1021/acsnano.0c00326
ACS Nano 2020, 14, 5711−5727

100 kDa pABOL group only reached a titer of ∼100 ng/mL, whereas the 8 kDa pABOL and PEI groups reached titers of ∼8000 and ∼2000 ng/mL, respectively. Compared to the IM injections, the ID injection groups were less protective against influenza challenge. Only the 1 μg PEI group conferred complete protection and resulted in ∼12% weight loss during peak viremia. The 1 μg 8 kDa pABOL had ∼20% weight loss after 5 days and only reached antibody titers of ∼500 ng/mL. The 0.1 μg PEI, 0.1 μg 8 kDa pABOL, and 1/0.1 μg 100 kDa pABOL groups all had approximately equivalent antibody titers, never reaching more than ∼100 ng/mL and exhibiting low survival (Figure S16b). The hemagglutinin inhibition (HAI) (Figure 7e,f) and virus neutralization (Figure 7g,h) mirror the antibody titers. The 1 μg 8 kDa pABOL IM group had the highest HAI titer (∼500) and was the only group significantly higher than the naïve ($p = 0.0082$). Interestingly, both the 1 μg 8 and 100 kDa pABOL IM groups had significantly higher IC_{50} levels than the unvaccinated control group, with IC_{50} values of 2700 and 1800 and $p = 0.0057$ and 0.0180, respectively. These HAI and neutralization titers are higher than those observed for a similar dose of saRNA (1.25 μg) as reported by Vogel *et al.* in a similar influenza challenge model wherein the RNA was complexed with PEI.[13] We further tested whether varying the molecular weight of pABOL from 5 kDa to 100 kDa impacted the immunogenicity (Figure S17). We observed that increasing the molecular weight of pABOL beyond 5 kDa greatly enhanced the immunogenicity, but that there was no added benefit beyond 8 kDa. Overall, the 8 kDa pABOL group exhibited the highest antibody levels against HA after IM injection and conferred complete protection against flu challenge, even at a dose of only 0.1 μg. These results show that route of administration (IM *vs* ID) greatly influences the immunogenicity of polyplex-based vaccines. It is interesting to note that differences in immunogenicity for HA saRNA between PEI and higher molecular weight pABOLs were less marked than the differences in protein expression (Figure 4). Such differences have previously been observed for both saRNA[36,37] and mRNA vaccine formulations.[38,39] In this respect, the increased levels of protein expression mediated by higher molecular weight pABOL (Figure 4) may be advantageous for the delivery of biotherapeutics, while providing the flexibility to increase immunogenicity and specificity through the co-delivery of molecular adjuvants.[40]

CONCLUSIONS

Here we show that pABOL is an efficient delivery vehicle for saRNA both *in vitro* and *in vivo*. We show that increasing the molecular weight of a cationic, bioreducible polymer above 5 kDa enhances the delivery efficiency for saRNA. By using TEA as a catalyst during the polymer synthesis, we were able to achieve higher molecular weight polymers, up to 167 kDa, which resulted in enhanced delivery and immunogenicity. We show that saRNA formulated with pABOL results in ∼100-fold higher protein expression *in vivo* and a higher percentage of cells expressing saRNA both *ex vivo* in human skin explants and *in vivo* in mice after ID and IM injections than commercially available PEIs. The optimized titration method yields polyplexes that can be facilely sterilized using 0.2 μm syringe filters without jeopardizing the transfection efficiency *in vitro* or *in vivo*. Due to the scalability of polymer synthesis and ease of formulation preparation, the efficient uptake and expression in human skin explants, and immunogenicity and protection against flu challenge of pABOL formulations *in vivo*, we anticipate that this polymer is highly clinically translatable as a delivery vehicle for saRNA for both vaccines and therapeutics.

METHODS

Materials. All solvents and reagents were obtained from commercial sources (Aldrich and Fisher) and used as received unless stated otherwise. Dialysis tubing (14 kDa molecular weight cutoff) was obtained from BioDesign Inc. of New York. Syringe filters with a hydrophilic PVDF membrane were purchased from Sigma-Aldrich (UK).

Characterization. *Size Exclusion Chromatography (SEC).* The molecular weights and dispersities were characterized using an Agilent PL GPC-50 instrument, equipped with a refractive index (RI) detector, with HPLC grade DMF (containing 0.075 wt % LiBr) as the eluent at a flow rate of 1.0 mL min^{-1} at 40 °C. Two GRAM Linear columns were used in series. Near monodisperse poly(methyl methacrylate) standards were used to calibrate the instrument. The poly(amino amide)s were dissolved in HPLC grade DMF, containing 0.075 wt % LiBr, and filtered through 0.2 μm syringe filters prior to analysis. Crude polymers were used for SEC characterization unless stated otherwise.

Nuclear Magnetic Resonance. ^{1}H, $^{13}C\{^{1}H\}$, $^{1}H-^{1}H$ COSY, and $^{1}H-^{13}C$ HSQC NMR spectra were recorded using a Bruker AV 400 MHz spectrometer at room temperature.

Dynamic Light Scattering. Dynamic light scattering was used to determine the hydrodynamic diameter (D_h) and polydispersity of the nanostructures formed between pABOLs and saRNA, in buffer solutions (20 mM HEPES, 5 wt % glucose in water, pH 7.4) and was measured using the Zetasizer Nano ZS instrument. The scattering angle was fixed at 173°. Data processing was carried out using cumulant analysis of the experimental correlation function, and the Stokes−Einstein equation was used to calculate the hydrodynamic radii. All solutions were analyzed using disposable polystyrene cuvettes.

Zeta Potential. Zeta potential measurements were also conducted at 25 °C using a ZETASIZER Nano ZS instrument.

UV−Vis Spectroscopy. The saRNA recovery was monitored using a Nanodrop One (Thermo Fisher) before and after sterile filtration of the polyplexes, through a 0.2 μm syringe filter (membrane material: hydrophilic PVDF).

$$\text{saRNA recovery} = 100\% \times \frac{\text{saRNA}_{\text{detected}}}{\text{saRNA}_{\text{input}}}$$

Mass Spectroscopy. The byproduct of pABOL reduction was characterized using a Waters LCT Premier mass spectrometer. Samples were ionized using electrospray ionization (ESI).

Transmission Electron Microscopy. TEM was used to image polyplexes that were prepared in H_2O. A 10 μL sample was pipetted directly onto a holey carbon film grid with 300 mesh copper (Agar Scientific, UK) and stained with 2% (w/w) uranyl acetate, washed twice with DI H_2O, and allowed to air-dry. Samples were then imaged on a TEM-2100 Plus electron microscope (JEOL USA, Peabody, MA, USA) using a voltage of 80 kV.

Improved Synthesis Procedure of pABOLs. pABOL was synthesized by aza-Michael polyaddition of 4-amino-1-butanol (ABOL) to *N,N′*-cystaminebis(acrylamide) (CBA). In a typical experiment, CBA (221.0 mg, 0.848 mmol), ABOL (78 μL, 0.840 mmol), and triethylamine (12 μL, 0.084 mmol) were added into an ampule flask charged with a stir bar. A mixed solvent, MeOH/water (176 μL, 4/1, v/v), was also added into the ampule flask. Polymerization was carried out in the dark at 45 °C under a static nitrogen atmosphere. The reaction mixture became clear in less than 2 h. The mixture was allowed to react for 5 to 14 d (depending on the targeted molecular weight) to yield a highly viscous solution. Aliquots were taken at predetermined time intervals for ^{1}H NMR and SEC to monitor the conversion and molecular weight. The

https://dx.doi.org/10.1021/acsnano.0c00326
ACS Nano 2020, 14, 5711−5727

reaction was stopped by MeOH dilution (50 mL) once the targeted molecular weight was reached. The diluted reaction mixture was then acidified with 1.0 M HCl to pH ∼4 and then purified by dialysis (molecular weight cutoff = 3.5 kDa) against acidic water (4.0 L, pH ∼5, refreshed 6 times in 3 d). The polymers in their HCl-salt form were collected as a white solid after freeze-drying.

Synthesis of Fluorescently Labeled pABOL. pABOL-8, 45, or 100 (50 mg) was dissolved in DMF (2 mL) in a vial charged with a stir bar, and 20 μL of TEA was added to promote dissolution of the pABOL chains. Then, fluorescein isothiocyanate (FITC) (1 mg, 1.140×10^{-3} mmol) dissolved in 100 μL of DMF was added into the polymer solution. The mixture was allowed to react in the dark at 25 °C for 24 h. The reaction mixture was then dialyzed (molecular weight cutoff = 3.5 kDa) in the dark against acidic water (500 mL, pH ∼5, refreshed 6 times in 3 days). The labeled pABOL was collected as a yellow solid after freeze-drying.

Reduction of pABOL in the Presence of GSH. pABOL and GSH were dissolved in D_2O in a vial charged with a stir bar. The molar ratio of [S−S]/[GSH] = 1:10. The mixture was allowed to react at 37 °C for 24 h. Aliquots were taken at predetermined time intervals for ^{1}H NMR and mass spectroscopy to determine conversion. After complete reduction of the disulfide bond, HPLC was employed to separate GSH, glutathione disulfide (GSSG), and the degradation products, using a mixed solvent of MeCN (with 0.1% TFA) and H_2O (with 0.1% TFA) at a flow rate of 10 mL/min using a Shimadzu HPLC instrument. The MeCN content of the mixed solvent was increased on a gradient profile from 5% to 30% in 15 min.

***In Vitro* Transcription of saRNA.** Self-amplifying RNA encoding firefly luciferase, enhanced green fluorescent protein, or hemagglutinin from the H1N1 A/California/07/2009 strain and the replicase derived from VEEV was produced using *in vitro* transcription. pDNA was transformed into 5α *E. coli* (New England BioLabs, UK), cultured in 100 mL of Luria Broth (LB) with 100 μg/mL carbenicillin (Sigma-Aldrich, UK) and isolated using a Plasmid Plus MaxiPrep kit (QIAGEN, UK). The concentration and purity of pDNA was measured on a NanoDrop One (ThermoFisher, UK) and subsequently linearized using MluI for 3 h at 37 °C. For *in vitro* transfections, capped RNA was synthesized using 1 μg of linearized DNA template in an mMessage mMachine reaction (Ambion, UK) and purified using a MEGAClear column (Ambion, UK) according to the manufacturer's protocol. RNA for *in vivo* experiments was prepared as previously described.[41] Briefly, uncapped *in vitro* RNA transcripts were prepared using 1 μg of linearized DNA template in a MEGAScript reaction (Ambion, UK) according to the manufacturer's protocol. Transcripts were then purified by overnight by LiCl precipitation at −20 °C, pelleted by centrifugation at 14 000 rpm for 20 min at 4 °C, washed 1× with 70% EtOH, centrifuged at 14 000 rpm for 5 min at 4 °C, and then resuspended in UltraPure H_2O (Ambion, UK). Purified transcripts were then capped using the ScriptCap m7G capping system (CellScript, Madison, WI, USA) and ScriptCapt 2′-*O*-methyltransferase kit (CellScript) simultaneously according to the manufacturer's protocol. Capped transcripts were then purified by LiCl precipitation as detailed above, resuspended in UltraPure H_2O, and stored at −80 °C until further use.

Polyplex Formation between pABOL and saRNA. Stock solutions of PEI, pABOLs, and saRNA were prepared first by directly dissolving these materials in molecular grade water and stored at 4 °C for up to 3 months. The concentrations of the stock solutions are 2.00 μg/μL (PEI), 0.24 μg/μL (fLuc Mut RepRNA), and 5.00 μg/μL (pABOLs, *in vitro* studies) or 50 μg/μL (pABOLs, *in vivo* studies), respectively. Polyplexes were prepared using two methods: (a) "direct mixing" and (b) "titration". In order to compare how the MW and the ratio of polymer:saRNA affects transfection efficiency and protein expression, the mass of RNA in each sample was kept constant.

a. Direct Mixing. In a typical procedure, 4.17 μL of the saRNA stock solution was diluted to 200 μL using HEPES buffer (20 mM HEPES, 5 wt % glucose in water, pH 7.4). A predetermined amount of polymer stock solution was also diluted to 800 μL using the same buffer. Each tube was vortexed to ensure homogeneity. Then, the polymer buffer solution was added to the saRNA buffer solution rapidly, following by vortexing for 20 s to form the polyplex. A series of pABOL polyplex solutions were prepared with polymer:saRNA ratios ranging from 1:1 to 60:1 (w/w). PEI MAX was formulated at a polymer:saRNA ratio of 5:1, while jetPEI was formulated at an N:P ratio of 8:1 according to the manufacturer's protocol.

b. Titration. In a typical procedure, 4.17 μL of the saRNA stock solution was diluted to 800 μL using HEPES buffer (20 mM HEPES, 5 wt % glucose in water, pH 7.4). A predetermined amount of polymer stock solution was also diluted to 200 μL using the same buffer in centrifuge tubes, equipped with stir bars. Each tube was placed on a stir plate and stirred at 1200 rpm at ambient temperature. Then, the RNA solution was added to the polymer solution at a rate of 160 μL/min (unless otherwise stated). A series of pABOL polyplex solutions were prepared with polymer/saRNA ratios ranging from 1:1 to 60:1 (w/w).

Protocols for *in Vitro* Transfection Studies. Transfections were performed in HEK293T.17 cells (ATCC, USA) that were maintained in culture in complete Dulbecco's modified Eagle's medium (cDMEM) (Gibco, Thermo Fisher, UK) containing 10% (v/v) fetal calf serum (FCS), 5 mg/mL L-glutamine, and 5 mg/mL penicillin/streptomycin (Thermo Fisher, UK). Cells were plated at a density of 50 000 cells per well in a clear 96-well plate 24 h prior to transfection. For the transfection, the medium was completely removed and replaced with 50 μL of prewarmed transfection medium (DMEM with 5 mg/mL L-glutamine). A 100 μL amount of the polyplex solution was added to each well and allowed to incubate for 4 h; then the transfection medium was completely removed and replaced with 100 μL of cDMEM. After 24 h from the initial transfection, 50 μL of medium was removed from each well and 50 μL of ONE-Glo D-luciferin substrate (Promega, UK) was added and mixed well by pipetting. The total volume was transferred to a white 96-well plate (Costar) and analyzed on a FLUOstar Omega plate reader (BMG LABTECH, UK), and background fluorescence from the medium control wells was subtracted. For the glutathione inhibition assay, cells were incubated with 200 μM buthionine sulfoximine, a known glutathione inhibitor,[42] for 4 h prior to the transfection, and then the transfection was performed as detailed above.

Cytotoxicity and Endotoxin Burden of Polyplexes. For analysis of polyplex cytotoxicity, cells were transfected with 100 ng of saRNA complexed with varying ratios of pABOL and PEI to saRNA ranging from 10:1 to 450:1 (w/w) according to the above protocol. Twenty-four hours after the initial transfection, 20 μL of CellTiter-Blue reagent (Promega, UK) was added to each well and allowed to incubate for 1 h. The plate was then analyzed for absorbance on a FLUOstar Omega plate reader (BMG LABTECH, UK) and normalized to the medium control. The endotoxin in each sample was quantified using a Pierce Chromogenic Endotoxin Quant kit (ThermoScientific, UK) according to the manufacturer's protocol.

Confocal Microscopy. HEK 293 cells (ATCC, USA) were plated on an eight-well μ-Slide (ibidi, Germany) at a density of 10 000 cells per well 24 h prior to transfection. Polyplexes with FITC-labeled PEI, pABOL-8, pABOL-45, or pABOL-100 were prepared and added to the cells for 4 h. After 1 h the cells were washed 2× with PBS for 5 min and fixed in 4% paraformaldehyde (PFA). The membrane was then stained with 0.4% (v/v) wheat germ agglutinin (WGA)-555 (ThermoFisher, UK) for 30 min at RT and washed 2× with PBS, and then the nucleus was stained with 0.2% (v/v) Hoechst 33342 for 20 min at RT and then again washed 2× with PBS. Samples were stored at 4 °C until imaging on an SP8 inverted confocal microscope (Leica, Germany) using LAX X software (Leica, Germany). Images were merged using ImageJ (NIH, USA).

***In Vivo* fLuciferase Expression in Mice.** All animals were handled in accordance with the UK Home Office Animals Scientific Procedures Act 1986 and with an internal ethics board and UK government approved project (P63FE629C) and personal license (IC37CBB8F). Food and water were supplied *ad libitum*. Female

https://dx.doi.org/10.1021/acsnano.0c00326
ACS Nano 2020, 14, 5711−5727

BALB/c mice (Charles River, UK) 6−8 weeks of age were placed into groups (n = 5) and housed in a fully acclimatized room. *In vivo* imaging was performed as previously described.[43] Mice were injected either intramuscularly in both hind legs or intradermally with 5 μg of fLuc saRNA complexed with either pABOL or PEI in a total volume of 50 μL. After 7 days, the mice were injected intraperitoneally (IP) with 100 μL of XenoLight RediJect D-luciferin substrate (PerkinElmer, UK) and allowed to rest for 10 min. Mice were then anesthetized using isoflurane and imaged on an *In Vivo* Imaging System (IVIS) FX Pro (Kodak Co., Rochester, NY, USA) equipped with Molecular Imaging software version 5.0 (Carestream Health, USA) for 2 min. Signal from each injection site was quantified using Molecular Imaging software and expressed as relative light units (p/s).

Flow Cytometry Analysis of eGFP Expression in Human Skin Explants. Surgically resected specimens of human skin tissue were collected at Charing Cross Hospital, Imperial NHS Trust, London, UK. All tissues were collected after receiving signed informed consent from patients, under protocols approved by the Local Research Ethics Committee (MED_RS_11_014). The tissue was obtained from patients undergoing elective abdominoplasty or mastectomy surgeries and processed as previously described.[41] Briefly, tissue was refrigerated until arrival in the laboratory, where the subcutaneous layer of fat was removed, and the tissue was excised into 1 cm^2 sections. Explants were incubated at 37 °C with 5% CO_2 in Petri dishes with 10 mL of cDMEM with daily medium replacement. Explants were injected ID using a Micro-Fine Demi 0.3 mL syringe (Becton Dickinson, UK) with 2 μg of eGFP saRNA complexed with pABOL or PEI in a volume of 100 μL. After 3 days, skin explants were minced well with scissors and incubated in 3 mL of DMEM supplemented with 1 mg/mL collagenase P (Sigma, UK) and 5 mg/mL Dispase II (Sigma, UK) for 4 h at 37 °C on a rotational shaker. Digests were then filtered through a 70 μm cell strainer and centrifuged at 1750 rpm for 5 min. Cells were then resuspended in 1 mL of FACS buffer (PBS + 2.5% FCS) at a concentration of 1 × 10^7 cells/mL. A 100 μL amount of cell suspension was added to a FACS tube and stained with Fixable Aqua Live/Dead Cell stain (Thermo Fisher, UK) dilution 1:400 in FACS buffer for 20 min on ice. Cells were then washed with 2.5 mL of FACS buffer, centrifuged at 1750 rpm for 5 min, and stained for 30 min with a panel of antibodies to identify each cell type, as described previously.[41] Cells were then washed with 1 mL of FACS buffer, centrifuged at 1750 rpm for 5 min, and resuspended in 250 μL of PBS. Cells were fixed by addition of 250 μL of 3.0% paraformaldehyde for a final concentration of 1.5% and refrigerated until flow cytometry analysis. Samples were analyzed on an LSRFortessa (BD Biosciences, UK) flow cytometer with FACSDiva software (BD Biosciences, UK) with 100 000 acquired live cell events. Gating was performed as previously described.[41] Phenotypic identity of GFP-positive cells was quantified using FlowJo version 10 (FlowJo LLC, OR, USA).

Flow Cytometry Analysis of eGFP Expression in Murine Skin and Muscle. Female BALB/c mice (Charles River, UK) 6−8 weeks of age were placed into groups (n = 5) and housed in a fully acclimatized room. Mice were injected IM in both hind legs or ID with 5 μg of eGFP saRNA complexed with pABOL or PEI in a total volume of 50 μL. After 7 days, the mice were euthanized, and the muscle or skin around the injection site was excised and put in 3 mL of DMEM supplemented with 1 mg/mL collagenase P (Sigma, UK) and 5 mg/mL Dispase II (Sigma, UK) for 4 h at 37 °C on a rotational shaker. Digests were then filtered through a 70 μm cell strainer and centrifuged at 1750 rpm for 5 min. Cells were then resuspended in 1 mL of FACS buffer (PBS + 2.5.% FCS) at a concentration of 1 × 10^7 cells/mL. A 100 μL sample of cell suspension was added to a FACS tube and stained with Fixable Aqua LIVE/DEAD Cell stain (Thermo Fisher, UK) dilution 1:400 in FACS buffer for 20 min on ice. Cells were then washed with 1 mL of FACS buffer, centrifuged at 1750 rpm for 5 min, and resuspended in 250 μL of PBS. Cells were fixed by addition of 250 μL of 3.0% paraformaldehyde for a final concentration of 1.5% and refrigerated until flow cytometry analysis. Samples were analyzed on a LSRFortessa (BD Biosciences, UK) flow cytometer with FACSDiva software (BD Biosciences, UK) with 100 000 acquired live cell events. Gating strategy was performed as previously reported.[41] Phenotypic identity of GFP-positive cells was quantified using FlowJo version 10 (FlowJo LLC, OR, USA).

***Ex Vivo* fLuciferase Expression in Human Skin Explants.** Human skin tissue was collected and excised as described above. Explants were incubated at 37 °C with 5% CO_2 in Petri dishes with 10 mL of cDMEM. Medium was replaced daily. Explants were injected ID using a Micro-Fine Demi 0.3 mL syringe (Becton Dickinson, UK) with 2 μg of fLuc saRNA complexed with pABOL or PEI in a volume of 100 μL. After 3 days, skin explants were inverted and the medium was replaced with 5 mL of cDMEM supplemented with 100 μL of XenoLight RediJect D-luciferin substrate (PerkinElmer, UK) and imaged on an IVIS FX Pro (Kodak Co., Rochester, NY, USA) equipped with Molecular Imaging software version 5.0 (Carestream Health, USA) for 60 min. Signal from each injection site was quantified using Molecular Imaging software and expressed as relative light units (p/s).

***In Vivo* Immunogenicity of HA saRNA.** BALB/c mice were immunized IM in one hind leg with either 1 or 0.1 μg of HA saRNA formulated with either *in vivo* jetPEI, pABOL-8 (Table 1, #2), or pABOL-100 (Table 1, #8) in a total volume of 50 μL and boosted after 6 weeks. Blood was collected after 3, 6, and 9 weeks from study onset *via* tail bleeding and centrifuged at 10 000 rpm for 5 min, and then the serum was removed and stored at −80 °C until further use.

HA-Specific ELISA. A semiquantitative immunoglobulin ELISA protocol was performed as previously described.[44] Briefly, 0.5 μg/mL of HA-coated ELISA plates was blocked with 1% (w/v) BSA/0.05% (v/v) Tween-20 in PBS. After washing, diluted serum samples were added to the plates, incubated for 2 h, and washed, and a 1:4000 dilution of anti-mouse IgG-HRP (Southern Biotech, UK) was used. Standards were prepared by coating ELISA plate wells with anti-mouse Kappa (1:1,000) and Lambda (1:1,000) light chain (Serotec, UK), blocking with PBS/1% (w/v) BSA/0.05% (v/v) Tween-20, washing, and adding purified IgG (Southern Biotech, UK) starting at 1000 ng/mL and titrating down with a 5-fold dilution series. Samples and standards were developed using TMB (3,3′;5,5′-tetramethylbenzidine), and the reaction was stopped after 5 min with stop solution (Insight Biotechnologies, UK). Absorbance was read on a spectrophotometer (VersaMax, Molecular Devices) with SoftMax Pro GxP v5 software.

Influenza Challenge. Three weeks after the boost injection, mice were challenged with 4.2 × 10^5 pfu of influenza (Cal/09) suspended in 100 μL of PBS. Mice were anesthetized using isoflurane, challenged IN, and weighed each day to determine weight loss. According to the challenge protocol humane end-points, mice were euthanized if they sustained more than 3 days of 20% weight loss or 1 day of 25% weight loss.

Hemagglutinin Inhibition (HAI) Assay. HAI was performed on week 9 serum samples as previously described.[45] Briefly, sera was incubated with receptor-destroying enzyme (RDE II) (Denka Seiken Co.) at a ratio of 3 volumes of RDE to 1 volume sera, incubated at 37 °C for 16 h, and then heat inactivated at 56 °C for 30 min. Then, 6 volumes of serum-free DMEM supplemented with 1 μg/mL TPCK-trypsin (Thermo) was added to each sample, subsequently serially diluted 1:2 (v/v) in PBS to a final volume of 25 μL, and combined with 25 μL of working virus solution (4 HAU/25 μL). PBS was used as a negative control, and virus was used as a positive control. The plates were incubated at RT for 30 min, and then 50 μL of 0.5% red blood cells (v/v) (turkey blood in Alsevers, ENVIGO) was added to each well and allowed to settle for 30 min at RT. The HAI titer was then recorded for each well, which was defined as the highest dilution that causes complete inhibition of hemagglutination.

Influenza Microneutralization Assay. Influenza microneutralization was performed on week 9 serum samples as previously described.[46] Briefly, MDCK cells were seeded at 10 000 cells/well in cDMEM in a 96-well plate. Sera was prepared with RDE and TPCK-trypsin, heat-inactivated as detailed in the HAI assay above, and then

https://dx.doi.org/10.1021/acsnano.0c00326
ACS Nano 2020, 14, 5711−5727

diluted in 1:5 serial dilution in serum-free DMEM supplemented with penicillin/streptomycin, L-glutamine, and 1 μg/mL TPCK-trypsin. Samples were then diluted with an equal volume of virus at a concentration of 100 $TCID_{50}$ in 50 μL, incubated for 1 h at 37 °C, and then added to MDCK cells and cultured for 24 h at 37 °C. Cells were then fixed with cold 80% acetone (v/v) and quantified using an influenza nucleoprotein ELISA. Plates were blocked with 5% (w/v) nonfat milk in PBS + 0.05% (v/v) Tween20 for 1 h, then treated with rabbit anti-NP antibody (Thermo) diluted 1:1000 for 1 h and mouse anti-rabbit IgG-HRP (Santa Cruz) diluted 1:5000 for 1 h. Plates were developed using TMB solution for 5 min at RT and then stop solution and read at OD_{450}/OD_{800}; the IC_{50} was calculated for each sample.

Statistical Analysis. Graphs and statistics were prepared in GraphPad Prism, version 8. Statistical differences were analyzed using either a two-tailed *t* test or an ordinary one-way ANOVA with multiple comparisons, with $p < 0.05$ used to indicate significance.

Data Availability. Raw data are available upon reasonable request from rdm-enquiries@imperial.ac.uk.

ASSOCIATED CONTENT

Supporting Information

The Supporting Information is available free of charge at https://pubs.acs.org/doi/10.1021/acsnano.0c00326.

Additional information (PDF)

AUTHOR INFORMATION

Corresponding Authors

Robin J. Shattock − *Department of Infectious Diseases, Imperial College London, London W2 1PG, U.K.*; Email: r.shattock@imperial.ac.uk

Molly M. Stevens − *Department of Materials, Department of Bioengineering, Institute of Biomedical Engineering, Imperial College London, London SW7 2AZ, U.K.; Department of Medical Biochemistry and Biophysics, Karolinska Institutet, Stockholm 171 65, Sweden*; orcid.org/0000-0002-7335-266X; Email: m.stevens@imperial.ac.uk

Authors

Anna K. Blakney − *Department of Infectious Diseases, Imperial College London, London W2 1PG, U.K.*; orcid.org/0000-0002-5812-9689

Yunqing Zhu − *Department of Materials, Department of Bioengineering, Institute of Biomedical Engineering, Imperial College London, London SW7 2AZ, U.K.; School of Materials Science and Engineering, Tongji University, Shanghai 200092, China*; orcid.org/0000-0002-2557-003X

Paul F. McKay − *Department of Infectious Diseases, Imperial College London, London W2 1PG, U.K.*

Clément R. Bouton − *Department of Infectious Diseases, Imperial College London, London W2 1PG, U.K.*

Jonathan Yeow − *Department of Materials, Department of Bioengineering, Institute of Biomedical Engineering, Imperial College London, London SW7 2AZ, U.K.*; orcid.org/0000-0003-3709-5149

Jiaqing Tang − *Department of Materials, Department of Bioengineering, Institute of Biomedical Engineering, Imperial College London, London SW7 2AZ, U.K.*

Kai Hu − *Department of Infectious Diseases, Imperial College London, London W2 1PG, U.K.*

Karnyart Samnuan − *Department of Infectious Diseases, Imperial College London, London W2 1PG, U.K.*

Christopher L. Grigsby − *Department of Medical Biochemistry and Biophysics, Karolinska Institutet, Stockholm 171 65, Sweden*

Complete contact information is available at: https://pubs.acs.org/10.1021/acsnano.0c00326

Author Contributions

§A.B. and Y.Z. are equal first authors, alphabetical order.

Author Contributions

A.K.B., Y.Z., P.F.M., C.L.G., R.J.S., and M.M.S. conceptualized and iterated the design of the polymer. A.K.B., Y.Z., and P.F.M. were responsible for the study design, guided by R.J.S. and M.M.S. Y.Z. and C.L.G. synthesized the polymers. A.K.B, J.T., Y.Z., and J.Y., designed and performed the *in vitro* experiments. C.R.B., K.H., and K.S. aided with *in vitro* experiments and preparation of RNA. A.K.B. and P.F.M. designed and performed the *in vivo* experiments. A.K.B. and Y.Z. wrote the manuscript with constructive feedback and editing from P.F.M., C.R.B., C.L.G., R.J.S., and M.M.S.

Notes

The authors declare the following competing financial interest(s): A.K.B., Y.Z., R.J.S., and M.M.S. are co-inventors on a patent resulting from this work.

ACKNOWLEDGMENTS

We gratefully acknowledge the surgeons at Charing Cross Hospital, E. Dex and J. Hunter, and their nursing team for providing the tissue used in these experiments. A.K.B. is supported by a Whitaker Post-Doctoral Fellowship and a Marie Skłodowska Curie Individual Fellowship funded by the European Commission H2020 (No. 794059). C.L.G. is supported by a Whitaker Post-Doctoral Fellowship. J.Y. was funded by the grant from the UK Regenerative Medicine Platform "Acellular/Smart Materials−3D Architecture" (MR/R015651/1). Y.Z., P.F.M., C.R.B., K.H., K.S., R.J.S., and M.M.S. are funded by the Department of Health and Social Care using UK Aid funding managed by the Engineering and Physical Sciences Research Council (EPSRC, grant number: EP/R013764/1, note: the views expressed in this publication are those of the author(s) and not necessarily those of the Department of Health and Social Care) and by Imperial College London's Wellcome Trust Institutional Strategic Support Fund (204834/Z/16/Z) as part of the Imperial Confidence in Concept scheme. M.M.S. and C.L.G. acknowledge support from the Swedish Research Council (VR 4-478/2016). We also acknowledge Dormeur Investment Services Ltd. for providing funds to purchase equipment used in these studies.

REFERENCES

(1) Ulmer, J. B.; Valley, U.; Rappuoli, R. Vaccine Manufacturing: Challenges and Solutions. *Nat. Biotechnol.* **2006**, *24*, 1377−1383.

(2) Petsch, B.; Schnee, M.; Vogel, A. B.; Lange, E.; Hoffmann, B.; Voss, D.; Schlake, T.; Thess, A.; Kallen, K.-J.; Stitz, L.; Kramps, T. Protective Efficacy of *In Vitro* Synthesized, Specific mRNA Vaccines against Influenza a Virus Infection. *Nat. Biotechnol.* **2012**, *30*, 1210.

(3) Guan, S.; Rosenecker, J. Nanotechnologies in Delivery of mRNA Therapeutics Using Nonviral Vector-Based Delivery Systems. *Gene Ther.* **2017**, *24*, 133.

(4) Karikó, K.; Muramatsu, H.; Welsh, F. A.; Ludwig, J.; Kato, H.; Akira, S.; Weissman, D. Incorporation of Pseudouridine into mRNA Yields Superior Nonimmunogenic Vector with Increased Transla-

tional Capacity and Biological Stability. *Mol. Ther.* **2008**, *16*, 1833−1840.
(5) Thess, A.; Grund, S.; Mui, B. L.; Hope, M. J.; Baumhof, P.; Fotin-Mleczek, M.; Schlake, T. Sequence-Engineered mRNA without Chemical Nucleoside Modifications Enables an Effective Protein Therapy in Large Animals. *Mol. Ther.* **2015**, *23*, 1456−1464.
(6) Kauffman, K. J.; Webber, M. J.; Anderson, D. G. Materials for Non-Viral Intracellular Delivery of Messenger Rna Therapeutics. *J. Controlled Release* **2016**, *240*, 227−234.
(7) Sahin, U.; Karikó, K.; Türeci, Ö. mRNA-Based Therapeutics — Developing a New Class of Drugs. *Nat. Rev. Drug Discovery* **2014**, *13*, 759−780.
(8) Perri, S.; Greer, C. E.; Thudium, K.; Doe, B.; Legg, H.; Liu, H.; Romero, R. E.; Tang, Z.; Bin, Q.; Dubensky, T. W.; Vajdy, M.; Otten, G. R.; Polo, J. M. An Alphavirus Replicon Particle Chimera Derived from Venezuelan Equine Encephalitis and Sindbis Viruses Is a Potent Gene-Based Vaccine Delivery Vector. *J. Virol.* **2003**, *77*, 10394−10403.
(9) Chahal, J. S.; Khan, O. F.; Cooper, C. L.; McPartlan, J. S.; Tsosie, J. K.; Tilley, L. D.; Sidik, S. M.; Lourido, S.; Langer, R.; Bavari, S.; Ploegh, H. L.; Anderson, D. G. Dendrimer-Rna Nanoparticles Generate Protective Immunity against Lethal Ebola, H1n1 Influenza, and Toxoplasma Gondii Challenges with a Single Dose. *Proc. Natl. Acad. Sci. U. S. A.* **2016**, *113*, E4133−E4142.
(10) Geall, A. J.; Verma, A.; Otten, G. R. Nonviral Delivery of Self-Amplifying Rna Vaccines. *Proc. Natl. Acad. Sci. U. S. A.* **2012**, *109*, 14604.
(11) Bogers, W. M.; Oostermeijer, H.; Mooij, P.; Koopman, G.; Verschoor, E. J.; David, D.; Ulmer, J. B.; Brito, L. A.; Cu, Y.; Banerjee, K.; Otten, G. R.; Burke, B.; Dey, A.; Heeney, J. L.; Shen, X.; Tomaras, G. D.; Labranche, C.; Montefiori, D. C.; Liao, H.; Haynes, B.; et al. Potent Immune Responses in Rhesus Macaques Induced by Non-Viral Delivery of a Self-Amplifying Rna Vaccine Expressing Hiv-1 Envelope with a Cationic Nanoemulsion. *J. Infect. Dis.* **2015**, *211*, 947.
(12) Brito, L. A.; Chan, M.; Shaw, C. A.; Hekele, A.; Carsillo, T.; Schaefer, M.; Archer, J.; Seubert, A.; Otten, G. R.; Beard, C. W.; Dey, A. K.; Lilja, A.; Valiante, N. M.; Mason, P. W.; Mandl, C. W.; Barnett, S. W.; Dormitzer, P. R.; Ulmer, J. B.; Singh, M.; O'Hagan, D. T.; et al. A Cationic Nanoemulsion for the Delivery of Next-Generation Rna Vaccines. *Mol. Ther.* **2014**, *22*, 2118−2129.
(13) Vogel, A. B.; Lambert, L.; Kinnear, E.; Busse, D.; Erbar, S.; Reuter, K. C.; Wicke, L.; Perkovic, M.; Beissert, T.; Haas, H.; Reece, S. T.; Sahin, U.; Tregoning, J. S. Self-Amplifying Rna Vaccines Give Equivalent Protection against Influenza to mRNA Vaccines but at Much Lower Doses. *Mol. Ther.* **2018**, *26*, 446−455.
(14) Blakney, A. K.; Yilmaz, G.; McKay, P. F.; Becer, C. R.; Shattock, R. J. One Size Does Not Fit All: The Effect of Chain Length and Charge Density of Poly(Ethylene Imine) Based Copolymers on Delivery of Pdna, mRNA, and Reprna Polyplexes. *Biomacromolecules* **2018**, *19*, 2870−2879.
(15) Kunath, K.; von Harpe, A.; Fischer, D.; Petersen, H.; Bickel, U.; Voigt, K.; Kissel, T. Low-Molecular-Weight Polyethylenimine as a Non-Viral Vector for DNA Delivery: Comparison of Physicochemical Properties, Transfection Efficiency and *In Vivo* Distribution with High-Molecular-Weight Polyethylenimine. *J. Controlled Release* **2003**, *89*, 113−125.
(16) Lin, C.; Zhong, Z.; Lok, M. C.; Jiang, X.; Hennink, W. E.; Feijen, J.; Engbersen, J. F. J. Novel Bioreducible Poly(Amido Amine)S for Highly Efficient Gene Delivery. *Bioconjugate Chem.* **2007**, *18*, 138−145.
(17) Chen, G.; Wang, K. K.; Hu, Q.; Ding, L.; Yu, F.; Zhou, Z. W.; Zhou, Y. W.; Li, J.; Sun, M. J.; Oupicky, D. Combining Fluorination and Bioreducibility for Improved Sirna Polyplex Delivery. *ACS Appl. Mater. Interfaces* **2017**, *9*, 4457−4466.
(18) Chen, G.; Wang, K. K.; Wang, Y. X.; Wu, P. K.; Sun, M. J.; Oupicky, D. Fluorination Enhances Serum Stability of Bioreducible Poly(Amido Amine) Polyplexes and Enables Efficient Intravenous Sirna Delivery. *Adv. Healthcare Mater.* **2018**, *7*, 1700978.
(19) Piest, M.; Lin, C.; Mateos-Timoneda, M. A.; Lok, M. C.; Hennink, W. E.; Feijen, J.; Engbersen, J. F. J. Novel Poly(Amido Amine)S with Bioreducible Disulfide Linkages in Their Diamino-Units: Structure Effects and *In Vitro* Gene Transfer Properties. *J. Controlled Release* **2008**, *130*, 38−45.
(20) Martello, F.; Piest, M.; Engbersen, J. F. J.; Ferruti, P. Effects of Branched or Linear Architecture of Bioreducible Poly(Amido Amine) S on Their *In Vitro* Gene Delivery Properties. *J. Controlled Release* **2012**, *164*, 372−379.
(21) Parmar, R. G.; Poslusney, M.; Busuek, M.; Williams, J. M.; Garbaccio, R.; Leander, K.; Walsh, E.; Howell, B.; Sepp-Lorenzino, L.; Riley, S.; Patel, M.; Kemp, E.; Latham, A.; Leone, A.; Soli, E.; Burke, R. S.; Carr, B.; Colletti, S. L.; Wang, W. Novel Endosomolytic Poly(Amido Amine) Polymer Conjugates for Systemic Delivery of Sirna to Hepatocytes in Rodents and Nonhuman Primates. *Bioconjugate Chem.* **2014**, *25*, 896−906.
(22) Emilitri, E.; Ranucci, E.; Ferruti, P. New Poly(Amidoamine)S Containing Disulfide Linkages in Their Main Chain. *J. Polym. Sci., Part A: Polym. Chem.* **2005**, *43*, 1404−1416.
(23) Burr, M. L.; Sparbier, C. E.; Chan, Y.-C.; Williamson, J. C.; Woods, K.; Beavis, P. A.; Lam, E. Y. N.; Henderson, M. A.; Bell, C. C.; Stolzenburg, S.; Gilan, O.; Bloor, S.; Noori, T.; Morgens, D. W.; Bassik, M. C.; Neeson, P. J.; Behren, A.; Darcy, P. K.; Dawson, S.-J.; Voskoboinik, I.; et al. Cmtm6Maintains the Expression of PD-L1 and Regulates Anti-Tumour Immunity. *Nature* **2017**, *549*, 101−105.
(24) Houtkooper, R. H.; Mouchiroud, L.; Ryu, D.; Moullan, N.; Katsyuba, E.; Knott, G.; Williams, R. W.; Auwerx, J. Mitonuclear Protein Imbalance as a Conserved Longevity Mechanism. *Nature* **2013**, *497*, 451−457.
(25) Stampfel, G.; Kazmar, T.; Frank, O.; Wienerroither, S.; Reiter, F.; Stark, A. Transcriptional Regulators Form Diverse Groups with Context-Dependent Regulatory Functions. *Nature* **2015**, *528*, 147−151.
(26) Delafosse, L.; Xu, P.; Durocher, Y. Comparative Study of Polyethylenimines for Transient Gene Expression in Mammalian Hek293 and Cho Cells. *J. Biotechnol.* **2016**, *227*, 103−111.
(27) Mann, J. F. S.; McKay, P. F.; Arokiasamy, S.; Patel, R. K.; Klein, K.; Shattock, R. J. Pulmonary Delivery of DNA Vaccine Constructs Using Deacylated Pei Elicits Immune Responses and Protects against Viral Challenge Infection. *J. Controlled Release* **2013**, *170*, 452−459.
(28) Wang, S. W.; Sen Gupta, A.; Sagnella, S.; Barendt, P. M.; Kottke-Marchant, K.; Marchant, R. E. Biomimetic Fluorocarbon Surfactant Polymers Reduce Platelet Adhesion on Ptfe/Eptfe Surfaces. *J. Biomater. Sci., Polym. Ed.* **2009**, *20*, 619−635.
(29) Lounis, F. M.; Chamieh, J.; Leclercq, L.; Gonzalez, P.; Geneste, A.; Prelot, B.; Cottet, H. Interactions between Oppositely Charged Polyelectrolytes by Isothermal Titration Calorimetry: Effect of Ionic Strength and Charge Density. *J. Phys. Chem. B* **2017**, *121*, 2684−2694.
(30) Varkouhi, A. K.; Scholte, M.; Storm, G.; Haisma, H. J. Endosomal Escape Pathways for Delivery of Biologicals. *J. Controlled Release* **2011**, *151*, 220−228.
(31) Miyata, K.; Nishiyama, N.; Kataoka, K. Rational Design of Smart Supramolecular Assemblies for Gene Delivery: Chemical Challenges in the Creation of Artificial Viruses. *Chem. Soc. Rev.* **2012**, *41*, 2562−2574.
(32) Tagde, A.; Singh, H.; Kang, M. H.; Reynolds, C. P. The Glutathione Synthesis Inhibitor Buthionine Sulfoximine Synergistically Enhanced Melphalan Activity against Preclinical Models of Multiple Myeloma. *Blood Cancer J.* **2014**, *4*, No. e229-e229.
(33) Bauhuber, S.; Hozsa, C.; Breunig, M.; Gopferich, A. Delivery of Nucleic Acids *Via* Disulfide-Based Carrier Systems. *Adv. Mater. (Weinheim, Ger.)* **2009**, *21*, 3286−3306.
(34) Kaczmarek, J. C.; Patel, A. K.; Kauffman, K. J.; Fenton, O. S.; Webber, M. J.; Heartlein, M. W.; DeRosa, F.; Anderson, D. G. Polymer-Lipid Nanoparticles for Systemic Delivery of mRNA to the Lungs. *Angew. Chem., Int. Ed.* **2016**, *55*, 13808−13812.

https://dx.doi.org/10.1021/acsnano.0c00326
ACS Nano 2020, 14, 5711−5727

(35) Liang, F.; Lindgren, G.; Lin, A.; Thompson, E. A.; Ols, S.; Röhss, J.; John, S.; Hassett, K.; Yuzhakov, O.; Bahl, K.; Brito, L. A.; Salter, H.; Ciaramella, G.; Loré, K. Efficient Targeting and Activation of Antigen-Presenting Cells *In Vivo* after Modified mRNA Vaccine Administration in Rhesus Macaques. *Mol. Ther.* **2017**, *25*, 2635−2647.
(36) Maruggi, G.; Zhang, C.; Li, J.; Ulmer, J. B.; Yu, D. mRNA as a Transformative Technology for Vaccine Development to Control Infectious Diseases. *Mol. Ther.* **2019**, *27*, 757−772.
(37) Pepini, T.; Pulichino, A.-M.; Carsillo, T.; Carlson, A. L.; Sari-Sarraf, F.; Ramsauer, K.; Debasitis, J. C.; Maruggi, G.; Otten, G. R.; Geall, A. J.; Yu, D.; Ulmer, J. B.; Iavarone, C. Induction of an Ifn-Mediated Antiviral Response by a Self-Amplifying Rna Vaccine: Implications for Vaccine Design. *J. Immunol.* **2017**, *198*, 1601877.
(38) Lutz, J.; Lazzaro, S.; Habbeddine, M.; Schmidt, K. E.; Baumhof, P.; Mui, B. L.; Tam, Y. K.; Madden, T. D.; Hope, M. J.; Heidenreich, R.; Fotin-Mleczek, M. Unmodified mRNA in Lnps Constitutes a Competitive Technology for Prophylactic Vaccines. *npj Vaccines* **2017**, *2*, 29.
(39) Hassett, K. J.; Benenato, K. E.; Jacquinet, E.; Lee, A.; Woods, A.; Yuzhakov, O.; Himansu, S.; Deterling, J.; Geilich, B. M.; Ketova, T.; Mihai, C.; Lynn, A.; McFadyen, I.; Moore, M. J.; Senn, J. J.; Stanton, M. G.; Almarsson, Ö.; Ciaramella, G.; Brito, L. A. Optimization of Lipid Nanoparticles for Intramuscular Administration of mRNA Vaccines. *Mol. Ther.–Nucleic Acids* **2019**, *15*, 1−11.
(40) Li, L.; Petrovsky, N. Molecular Mechanisms for Enhanced DNA Vaccine Immunogenicity. *Expert Rev. Vaccines* **2016**, *15*, 313−329.
(41) Blakney, A. K.; McKay, P. F.; Ibarzo Yus, B.; Hunter, J. E.; Dex, E. A.; Shattock, R. J. The Skin You Are In: Design-of-Experiments Optimization of Lipid Nanoparticle Self-Amplifying Rna Formulations in Human Skin Explants. *ACS Nano* **2019**, *13*, 5920−5930.
(42) Tagde, A.; Singh, H.; Kang, M. H.; Reynolds, C. P. The Glutathione Synthesis Inhibitor Buthionine Sulfoximine Synergistically Enhanced Melphalan Activity against Preclinical Models of Multiple Myeloma. *Blood Cancer Journal* **2014**, *4*, No. e229.
(43) Blakney, A. K.; McKay, P. F.; Christensen, D.; Yus, B. I.; Aldon, Y.; Follmann, F.; Shattock, R. J. Effects of Cationic Adjuvant Formulation Particle Type, Fluidity and Immunomodulators on Delivery and Immunogenicity of Sarna. *J. Controlled Release* **2019**, *304*, 65−74.
(44) Badamchi-Zadeh, A.; McKay, P. F.; Holland, M. J.; Paes, W.; Brzozowski, A.; Lacey, C.; Follmann, F.; Tregoning, J. S.; Shattock, R. J. Intramuscular Immunisation with Chlamydial Proteins Induces Chlamydia Trachomatis Specific Ocular Antibodies. *PLoS One* **2015**, *10*, No. e0141209.
(45) Zacour, M.; Ward, B. J.; Brewer, A.; Tang, P.; Boivin, G.; Li, Y.; Warhuus, M.; McNeil, S. A.; LeBlanc, J. J.; Hatchette, T. F. Standardization of Hemagglutination Inhibition Assay for Influenza Serology Allows for High Reproducibility between Laboratories. *Clin. Vaccine Immunol.* **2016**, *23*, 236.
(46) Grund, S.; Adams, O.; Wählisch, S.; Schweiger, B. Comparison of Hemagglutination Inhibition Assay, an Elisa-Based Micro-Neutralization Assay and Colorimetric Microneutralization Assay to Detect Antibody Responses to Vaccination against Influenza a H1n1 2009 Virus. *J. Virol. Methods* **2011**, *171*, 369−373.

https://dx.doi.org/10.1021/acsnano.0c00326
ACS Nano 2020, 14, 5711−5727